DIRECTIONAL EMISSIVITY MEASUREMENT

A Thesis

Presented to

the Faculty of Graduate Studies

University of Manitoba

In Partial Fulfillment

of the Requirements for the Degree

Master of Science

in Mechanical Engineering

by

Harry Alfred Hallewell

ABSTRACT

Investigations of the intensity of radiation in various directions from actual surfaces show that it does not follow the Lambert cosine law. Representative curves of non-conductors and conductors may be determined as shown in Figure 21 where ϵ_β is the ratio of the measured intensity of radiation at the angle β from a normal to the surface to the intensity of radiation from a black surface at the same temperature and angle β. It may be observed that ϵ_β is relatively constant for non-electrical conductors except in the neighborhood of 90° where it drops off sharply. On the other hand, ϵ_β for electrical conductors increases with β to a maximum very close to 90° and then decreases rapidly. For this reason, the total hemispherical emissivity of polished conductors may be from 1.15 to 1.20 times the total normal emissivity.[3] Values of total normal emissivities of various surfaces may have large variations for a single material depending primarily on the surface conditions.

The purpose of this project was to design and construct a reliable measuring apparatus to determine the angular emissivity of various materials within a temperature range of 150°F to 1000°F. Tests were not run at the maximum temperature quoted but a temperature of 840°F was reached on one particular test. Five different materials were tested under various surface temperatures. The results obtained compared favourably with published results. Total hemispherical emissivities were calculated for each test by means of graphical

integration. It may be noted that for the materials tested that the total hemispherical emissivity does not vary more than 15% from the total normal value obtained for any particular test.

It may be concluded that the apparatus performed satisfactorily and that it can be used to test other surfaces for which the angular emissivity is desired. Some minor changes were incorporated into the apparatus before the actual tests were begun. After completion of the tests and noting the bahaviour of the apparatus, some further refinements could be introduced which would increase the accuracy of the results obtained. These points are discussed in the main text of the thesis.

ACKNOWLEDGEMENTS

The writer wishes to express his gratitude to his advisor, Prof. D. W. Craik who suggested this research and offered many helpful suggestions, and to the National Research Council of Canada who donated money towards financing this project.

The writer is thankful to the technicians who helped construct the apparatus and all others involved in the program.

TABLE OF CONTENTS

LIST OF TABLES

LIST OF FIGURES

NOMENCLATURE

β - Angle of deviation from the normal to a surface-degree.

e - Emissive power of a body - $\frac{Btu}{hr.\ ft^2}$.

ϵ - Emissivity of a body or surface.

F - Shape factor of the radiometer fixed by the radiometer diaphragm size and arrangement.

i - Intensity of radiation - $\frac{Btu}{hr}$ per solid angle.

K - Constant of multiplication for finding hemispherical emissivity.

μ - micron, equals 1×10^{-4}cm.

q - radiant energy - $\frac{Btu}{hr}$.

σ - Stefan-Boltzmann constant $0.1714 \times 10^{-8} \frac{Btu}{hr\text{-}ft^2\text{-}R^{o4}}$.

T - Absolute temperature - ^{o}R.

θ - Angle measured on a surface from an arbitrary position. See Fig. 1.

w - Solid angle

G - Radiation flux density - $\frac{Btu}{hr\text{-}ft^2}$

SUBSCRIPTS

B	Black body	S	Sample
H	Hemisphere or hemispherical	R	Radiation
N	Normal (i.e. when $\beta = 0^{o}$)	C	Convection

I INTRODUCTION

This investigation was made possible by a grant provided by the National Research Council of Canada. The main purpose of the project was to design and construct an apparatus which was capable of measuring the directional emissive properties of various materials. In this way published emissivity values of common industrial materials could be checked and emissivities of special surfaces such as painted, corroded etc., could be determined whenever necessary. Before designing the apparatus, a literature search was executed to determine the parameters involved. Several types of apparatus have been constructed in recent years, one of which is at the University of Minnesota[1] and one at the Case Institute of Technology.[2] The apparatus described herein was designed with the following criteria:

(1) Radiometer readings were taken on a relative basis rather than absolute values. This tends to yield maximum accuracy results. It also tends to offset any aging characteristics which may occur and reduces effects of error caused by changing relative humidity.

(2) Because of small thermopile readings, an electronic amplifier was used. All final readings were taken on a portable potentiometer.

(3) All apparatus was built of non-corroding material to maintain long life and accuracy.

Numerous measurements were carried out in the late 1920's and 1930's by Schmidt and Eckert.[3] This data is still used today and provides a good comparison for results obtained from similar materials to those which they tested. Schmidt and Eckert[3] formulated theoretical equations for calculating the emissivity at a given angle for a given surface. This involves the electromagnetic theory which distinguishes two types of materials: electric conductors and non-conductors. For conductors, it establishes a relation between the radiation properties and the electrical resistivity, ρ_e, whereas for electrical non-conductors, the theory relates radiation properties to the refraction coefficient.

The total hemispherical emissivity is quite often required and not just the total normal emissivity. Definitions of these quantities follow later. In certain cases one value may be substituted directly for the other without involving any great error but this depends of course on what particular material is being considered. By investigating the directional properties of the surface and assuming these properties constant around the hemispheres, the total hemispherical emissivity may be calculated by means of a graphical integration.

II THEORY

The relative importance of several mechanisms of the transfer of heat from one body to another differs greatly with temperature. The phenomena of conduction and convection are affected primarily by temperature difference and very little by temperature level, whereas radiation interchange increases rapidly with an increase in temperature level. Therefore, at the higher temperatures radiation is usually the controlling factor in heat exchange.(6)

A different physical phenomenon is associated with radiation heat transfer than with either conduction or convection. The energy is transmitted through free space by electromagnetic waves at all wavelengths throughout the electromagnetic spectrum. Maximum transfer of heat occurs when the space is totally evacuated. All substances except perhaps some in outer space at absolute zero are continuously emitting electromagnetic waves at various wavelengths. Such waves are generated primarily by the movement of thermally agitated electrons in the atomic shell surrounding the atomic nuclei. These waves travel at the speed of light in a vacuum and when they impinge on another surface, produce corresponding electronic agitation and thereby effect a transfer of energy across the void. When a body is heated, radiant energy is emitted at a rate, and of a quantity, dependent primarily on the temperature of the body.(6)

Newton, Fresnel, Maxwell and others proposed different theories by which they anticipated radiation heat transfer occurred. Other theories were proposed near the end of the nineteenth century by

Michelson and Morley. Einstein's theory of relativity and Planck's quantum theory help to explain the phenomena of electromagnetic waves. What next will occur is difficult to imagine but the picture is by no means complete.[6]

The energy flow impinging per unit time on a unit area of a surface is called the incident radiation or irradiation and may be denoted by H.[3] Of this total quantity some is reflected, some is absorbed and some is transmitted.

$$\rho + \alpha + \tau = 1 \quad . \quad . \quad . \quad . \quad (1)$$

ρ = reflectivity

α = absorptivity

τ = transmissivity

The total radiant energy emitted per unit area of the surface per unit time is defined as the emissive power and is denoted by e. A body whose absorptivity is one is called a black body. There are no totally black surfaces in nature but one may be created artificially as will be explained later. They may be black to certain wavelengths but not completely black to all. "No surface radiates more heat than a black body." This is the content of Kirchhoff's law.

The ratio of the emissive power of any body to the emissive power of a black body at the same temperature is called the emissivity ϵ or to be more exact the total hemispherical emissivity.

i.e.
$$\epsilon_H = \frac{e_S}{e_B} \quad . \quad . \quad . \quad . \quad . \quad (2)$$

The total directional emissivity is defined as the ratio of the intensity of radiation at the angle β from a normal to the surface to the intensity of radiation from a black surface at the same temperature and angle.

i.e: $$\epsilon_\beta = \frac{i_S}{i_B} \text{ at angle } \beta \quad . \quad . \quad . \quad (3)$$

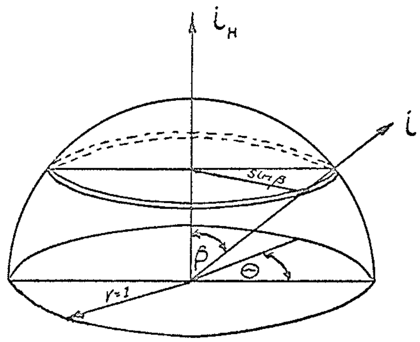

Figure 1

Determining Radiation in Different Directions.

Referring to Figure 1, the radiation intensity in the contemplated direction is defined as:

$$i = \frac{dq}{dw} \quad . \quad . \quad (4)$$

Radiation intensity i_B of a black body is given by Lambert's cosine law:

$$i_B = i_{B_N} \cos\beta \quad . \quad . \quad . \quad (5)$$

$$e_B = \int i_B \, dw = 2\pi i_{B_N} \int \cos\beta \, \sin\beta \, d\beta = \pi i_{B_N}$$

Now: $$\epsilon_H = \frac{e_S}{e_B} = \frac{\int_H i_S \, dw}{\pi i_{B_N}}$$

From Equation (3)

$$i_S = \epsilon_\beta \, i_B \text{ at angle } \beta$$

$$i_B = i_{B_N} \cos\beta$$

$$i_S = \epsilon_\beta \, i_{B_N} \cos\beta \quad . \quad . \quad . \quad . \quad . \quad . \quad (6)$$

Substituting:

$$\epsilon_H = \frac{1}{\pi}\int_H \epsilon_\beta \cos\beta \, dw$$

Referring to Figure 1 again:

$$dw = r\,d\beta\;R\,d\,\theta \qquad \text{where } R = r\sin\beta$$

$$dw = r^2\,d\beta\;d\,\theta\,\sin\beta \qquad r = 1$$

Substituting:

$$\epsilon_H = \frac{1}{\pi}\int_0^{\frac{\pi}{2}}\int_0^{2\pi}\epsilon_\beta \sin\beta\;\cos\beta\;d\beta\;d\,\theta \quad . \quad . \qquad (7)$$

If ϵ_β varies with θ then:

$$\epsilon_H = \frac{1}{\pi}\int_0^{\frac{\pi}{2}}\int_0^{2\pi}\epsilon_{\beta,\,\theta}\;\sin\beta\;\cos\beta\;d\beta\;d\,\theta \quad . \qquad (8)$$

Equation (8) was used to evaluate the total hemispherical emissivity for each of the tests performed. When the radiation intensity of a surface follows the same cosine law as black body radiation then the directional emissivity is independent of the angle β towards the surface normal and identical with the total hemispherical emissivity.

Solids and liquids absorb practically all incident energy of infrared wavelengths in very thin layers immediately below their surface and the emitted radiation leaving their surface also comes from such a thin layer. For conductors this layer is about 1μ thick and for non-conductors it may go as high as 0.1 in.[(3)] All solids and liquids reflect a fraction of impinging radiation and therefore radiate less energy than a black body. With respect to their thermal radiation properties in the infrared wavelength range, there is a principal difference between electrical conductors and non-conductors. The conductors reflect the major part of impinging radiation and therefore radiate comparatively little heat. Non-conductors absorb the major part of impinging radiation and radiate comparatively much heat. This rule does not apply to radiation in the visible or shorter wavelength range.[3] Radiation emitted from heated bodies usually comprises rays with wavelengths of one micron or more. This thermal radiation is comprised of waves outside the visible range and is generally called infra-red. For both groups of materials mentioned, the reflectivity, absorptivity and emissivity change with wavelength. A surface whose absorptivity is the same for all wavelengths is called a gray surface.

Emissivity depends sometimes to a considerable degree, on the surface conditions and it is often difficult to describe this condition precisely enough. Emissivity values depend also on the temperature. A general rule is that the emissivity increases with temperature for conductors and decreases with increasing temperature for non-conductors. From the total hemispherical emissivity ϵ_H, the heat radiated per unit area at the absolute temperature T can be calculated by the formula:

$$e = \epsilon \sigma T^4 \quad . \quad . \quad . \quad . \quad (9)$$

where e is the emissive power.

Information on the radiation properties of solids and liquids can be obtained from the electromagnetic theory.[3] This theory considers radiation as a combination of electric and magnetic waves and applies the laws for reflection of such waves on the interface of substances which differ in their electrical properties. It is found that predictions obtained by this theory are in fairly good agreement with experimental results so that they may be used as a guide to measure values which are not available as long as the radiation considered is primarily in the infrared region. For conductors the following equation was derived for the emissivity in a direction normal to the surface:

$$\epsilon_N = 0.576 \sqrt{\rho_e t} - 0.124 \rho_e t \quad . \quad . \quad (10)$$

where: ρ_e = ohm-centimeters

t = degrees Kelvin.

This usually agrees within 20% with measurements. Another useful relation was also obtained by Schmidt and Eckert[3] for the ratio ϵ_H/ϵ_N as shown in Figure 2.

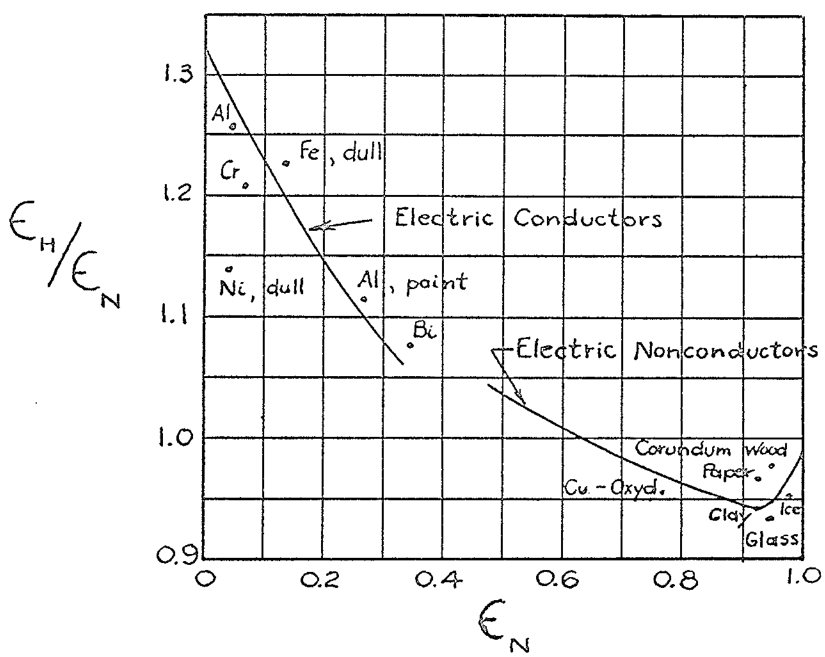

Figure 2. Ratio of Hemispherical to Normal Emissivities.

The curves in Figure 2 show as full lines the prediction of the theory for electric conductors and non-conductors. The points indicate measured results of Schmidt and Eckert.[3]

III RADIOMETER ENERGY EXCHANGE ANALYSIS

A general layout of the apparatus and measuring equipment is shown in Figures 3 and 12. With reference to the designed rig, the following analysis may be applied. A sample calculation for Test # 18 is contained in Appendix B. The equation used to calculate the angular emissivity was derived in a manner which best suited the means by which the emissivity data was obtained. A similar approach has been used by others on this same topic.[1] Assumptions made in the derivation are noted as they occur.

The radiant energy flux (G) leaving the black body at temperature T_B and arriving on a unit area of the thermopile is:

$$G_B = F \sigma T_B^4 \quad . \quad . \quad . \quad . \qquad (11)$$

The sample is at a temperature T_s and is completely surrounded by a nearly perfect black guard at temperature T_G which was taken as the average temperature between the inlet and outlet water temperatures to the base of the guard container.

The following energies arriving at a unit area of the thermopile were considered:

1. The emitted energy of the sample.
2. Energy coming from the guard and being reflected by the sample.
3. Energy coming from the guard after being reflected by the sample holder to the sample and in turn reflected to the thermopile.
4. Energy coming from the holder and reflected by the sample.
5. Energy originating from either the guard surface or the sample surface and reaching the thermopile after multiple reflections.

GENERAL ARRANGEMENT DRAWING

FIG 3

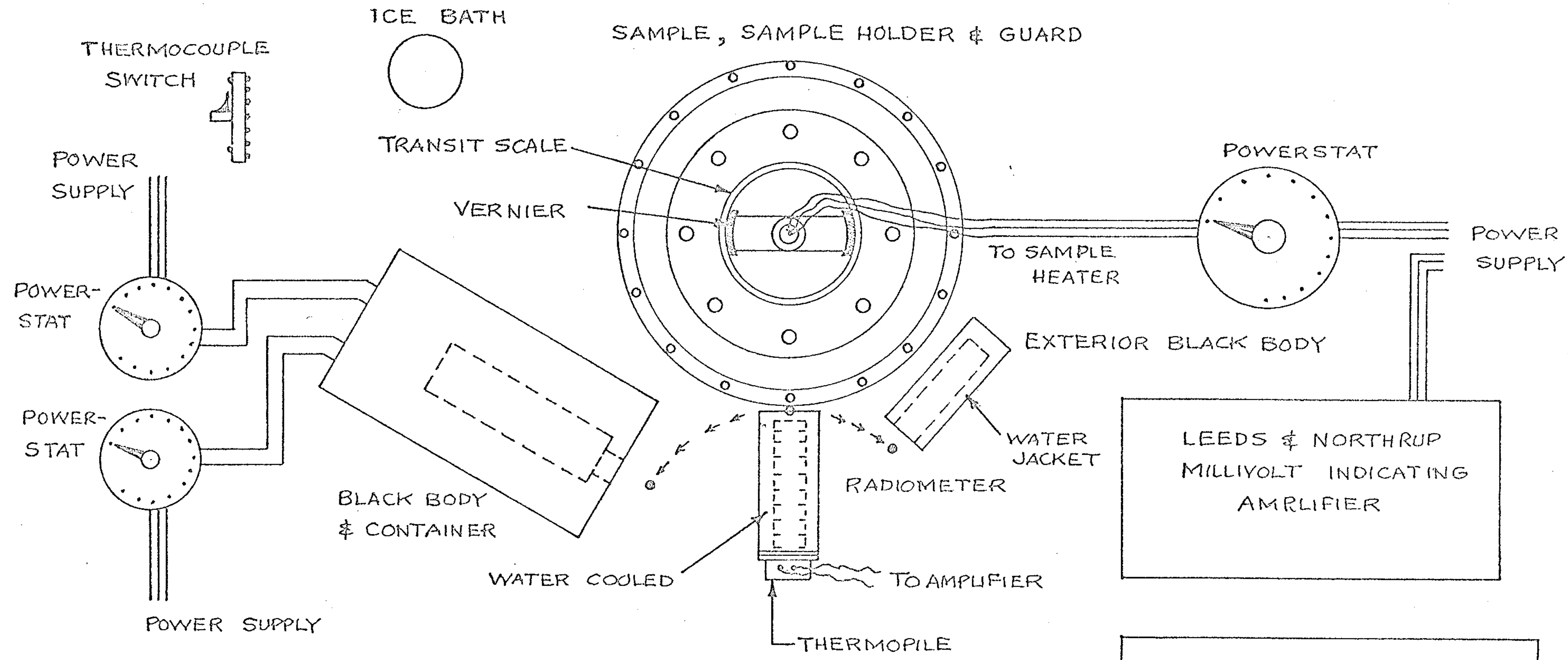

UNIVERSITY OF MANITOBA
DEPT OF MECH ENGINEERING
SCALE N.T.S. DATE JULY 22/63
DRWN HAH

Terms 3, 4, and 5 were neglected as it was assumed that the errors involved would be smaller than those anticipated in the actual measurements. Thus we may write:

$$G_s = F\sigma\left[\epsilon_s T_s^4 + \rho_s T_G^4\right] \quad . \quad . \quad . \quad (12)$$

The following substitution may be made:

$$1 - \rho_s = \epsilon_s$$

The assumption that $\epsilon_s = 1 - \rho_s$ requires $\tau_s = 0$ so that no energy comes through the sample from the assumbly and that the emissivity does not depend on wavelength since ϵ_s is substituted for τ_s.

The limitation that $\tau_s = 0$ was satisfied by all samples except the glass. This factor, discussed later under sample preparation, was assumed to be negligible in the temperature range that the glass was tested.

With respect to the second assumption, Eckert(3) states the following, "For a metal surface at T_s and for incident black radiation at T_i it can be demonstrated from electromagnetic theory that the following relations held, $\alpha = \epsilon(T_m)$ with $T_m = \sqrt{T_s T_i}$." It was found that the emissivity did not change any noticeable amount for low temperatures encountered and therefore the emissivity was very close to absorptivity in this temperature range. At higher temperatures the term containing ρ_s becomes negligible.

The above equation may also be written as

$$1 - \rho_{s,\beta} = \epsilon_{s,\beta}$$

The equation in this form also applies to the derivation but is dependent on the radiation from the inside of the guard container. In order that the equation hold at all angles of β, the radiation from the inside of the container must be diffuse. This is a reasonable assumption since the inside of the guard was painted with three coats of flat black paint which, according to tests, had a hemispherical emissivity slightly greater than 0.92. Any error that may be introduced occurs at very large angles of β.

$$G_s = F\sigma\left[\epsilon_s(T_s^4 - T_G^4) + T_G^4\right] \quad . \quad . \quad . \qquad (13)$$

The radiant energy flux leaving the guard black body at temperature T_G and arriving on a unit area of the thermopile is:

$$G_G = F\sigma T_G^4 \quad . \quad . \quad . \quad . \quad . \qquad (14)$$

Subtract Equation (14) from (11) and (13) and equate:

$$\frac{G_B - G_G}{T_B^4 - T_G^4} = F\sigma$$

$$\frac{G_s - G_G}{\epsilon_s(T_s^4 - T_G^4)} = F\sigma$$

$$\epsilon_s = \frac{T_B^4 - T_G^4}{T_s^4 - T_G^4}\left[\frac{G_s - G_G}{G_B - G_G}\right] \quad . \quad . \quad . \quad . \quad . \qquad (15)$$

To relate the radiation heat fluxes, G, to the thermopile deflection, Δ, a heat balance may be written for the front face of the thermopile for each energy flux input.

$$C_B G_B = \sigma\epsilon_T T_{FB}^4 - q_{rad} + q_{loss} \quad . \quad . \quad . \qquad (16)$$

$$C_s\, G_s = \sigma\, \epsilon_T\, T_{FS}^4 - q_{rad} + q_{loss} \quad . \quad . \quad . \quad (17)$$

$$C_G\, G_G = \sigma\, \epsilon_T\, T_{FG}^4 - q_{rad} + q_{loss} \quad . \quad . \quad . \quad (18)$$

where: C = loss factor accounting for absorption of energy by CO_2 and water vapour in the air. (Equal to 1 if no absorption occurs).

ϵ_T = emissivity of the thermopile

q_{rad} = radiant energy absorbed by the thermopile coming from surrounding walls.

q_{loss} = losses from the thermopile by convection and conduction.

T_F = temperature of the exposed thermopile surface.

If we assume $C_B = C_s = C_G$ and q_{rad} and q_{loss} remain constant we combine and arrange (16), (17) and (18) to get:

$$\frac{G_s - G_G}{G_B - G_G} = \frac{T_{FS}^4 - T_{FG}^4}{T_{FB}^4 - T_{FG}^4} \quad . \quad . \quad . \quad . \quad (19)$$

A good approximation for fourth power temperature differences is: (provided $T_1 \approx T_2$)

$$\frac{T_1^4 - T_2^4}{T_1 - T_2} = 4\, \bar{T}_M^3 \text{ where } T_M = \frac{T_1 + T_2}{2}$$

$$\frac{G_s - G_G}{G_B - G_G} = \frac{4\, \bar{T}_{FG}^4}{4\, \bar{T}_{FG}^4} \frac{(T_{FS} - T_{FG})}{(T_{FB} - T_{FG})} = \frac{T_{FS} - T_{FG}}{T_{FB} - T_{FG}} \quad . \quad (20)$$

It was verified later that the maximum deflection produced by the thermopile during testing was approximately 0.50 millivolts. Considering the sensitivity of a bismuth-silver thermocouple and the number of thermocouples involved (16), the temperature rise necessary to produce the above deflection was 0.71°F. Thus, the temperature differences in Equation (20) are very small and the approximation holds.

Assuming $C_B - C_S = C_G$ may not be valid in all cases since the absorptivity of carbon dioxide and water vapor depend strongly on wave length, the radiometer may be flushed with a non-absorbing gas if necessary.

The thermopile output causing the potentiometer deflection, Δ, is directly proportional to the difference in the thermopile hot junction temperature T_H and the cold junction temperature T_C. The radiometer is constructed to maintain T_C as constant as possible. Therefore, when the radiometer is viewing the various components, the deflections are:

$$\Delta_B = \text{const } (T_{FB} - T_C) \quad . \quad . \quad . \quad . \quad (21)$$

$$\Delta_S = \text{const } (T_{FS} - T_C) \quad . \quad . \quad . \quad . \quad (22)$$

$$\Delta_G = \text{const } (T_{FG} - T_C) \quad . \quad . \quad . \quad . \quad (23)$$

Substituting Equations (21), (22) and (23) into Equation (20) and combining with Equation (15) we obtain:

$$\frac{\Delta_S - \Delta_G}{\Delta_B - \Delta_G} = \frac{T_{FS} - T_{FG}}{T_{FB} - T_{FG}} = \frac{G_S - G_G}{G_B - G_G}$$

$$\epsilon_S = \frac{T_B^{\,4} - T_G^{\,4}}{T_S^{\,4} - T_G^{\,4}} \left[\frac{\Delta_S - \Delta_G}{\Delta_B - \Delta_G} \right] \quad . \quad . \quad . \quad (24)$$

One must justify viewing the sample at an angle while viewing the black body at a constant normal position. This may be done because the sample area viewed at various angles from 0° to 90° increases at the same rate as the intensity of radiation from the black body decreases.

i.e. By Lambert's cosine law for a black body:

$$i_B = i_{B_N} \cos \beta$$

and for the sample viewing area

$$A_\beta = \frac{A_N}{\cos \beta}$$

Thus, Equation (24) may be used to find the emissivity at any angle and may be rewritten as:

$$\epsilon_S = \frac{T_B^4 - T_G^4}{T_S^4 - T_G^4} \left[\frac{\Delta_S - \Delta_G}{\Delta_B - \Delta_G} \right] \quad . \quad . \quad (25)$$

Equation (25) was used for all emissivity calculations. To find the hemispherical emissivity Equation (8) was graphically integrated.

IV DESIGN AND DESCRIPTION OF APPARATUS

It may be noted that the main components of the apparatus were centrally located around the radiometer. The main pieces of apparatus which had to be designed and built were the black body, guard, sample holder and radiometer. In the following sub-sections the components are described in detail as to purpose, design, material used and physical size.

Radiometer

The radiometer is composed of a thermopile, a diaphragm assembly and a water cooled jacket, the latter two of which may be seen in Figures 4 and 15. The purpose of the diaphragms was to allow the receiver area to intercept a predetermined amount of impinging radiation and also determine the actual size of sample required. The water cooled jacket was necessary to give a constant temperature environment and to absorb any stray radiation from the surroundings.

The thermopile was supplied by Eppley Laboratory, Inc. and consisted of a 16 junction bismuth silver pile coated internally with lamp black. It had a special air case with a slide providing a shutter opening of 10.5 m. From a series of measurements performed by Eppley, the thermopile was calculated to develop a sensitivity of 0.300 micro-volts per micro watt per sq.cm. Because of the lack of necessary equipment we were unable to verify this figure but it was understood to refer to irradiation upon the receiver surface. This figure was not used in the thesis because relative figures were used rather than absolute

RADIOMETER & WATER JACKET ASSEMBLY FIG 4

THERMOPILE NOT SHOWN

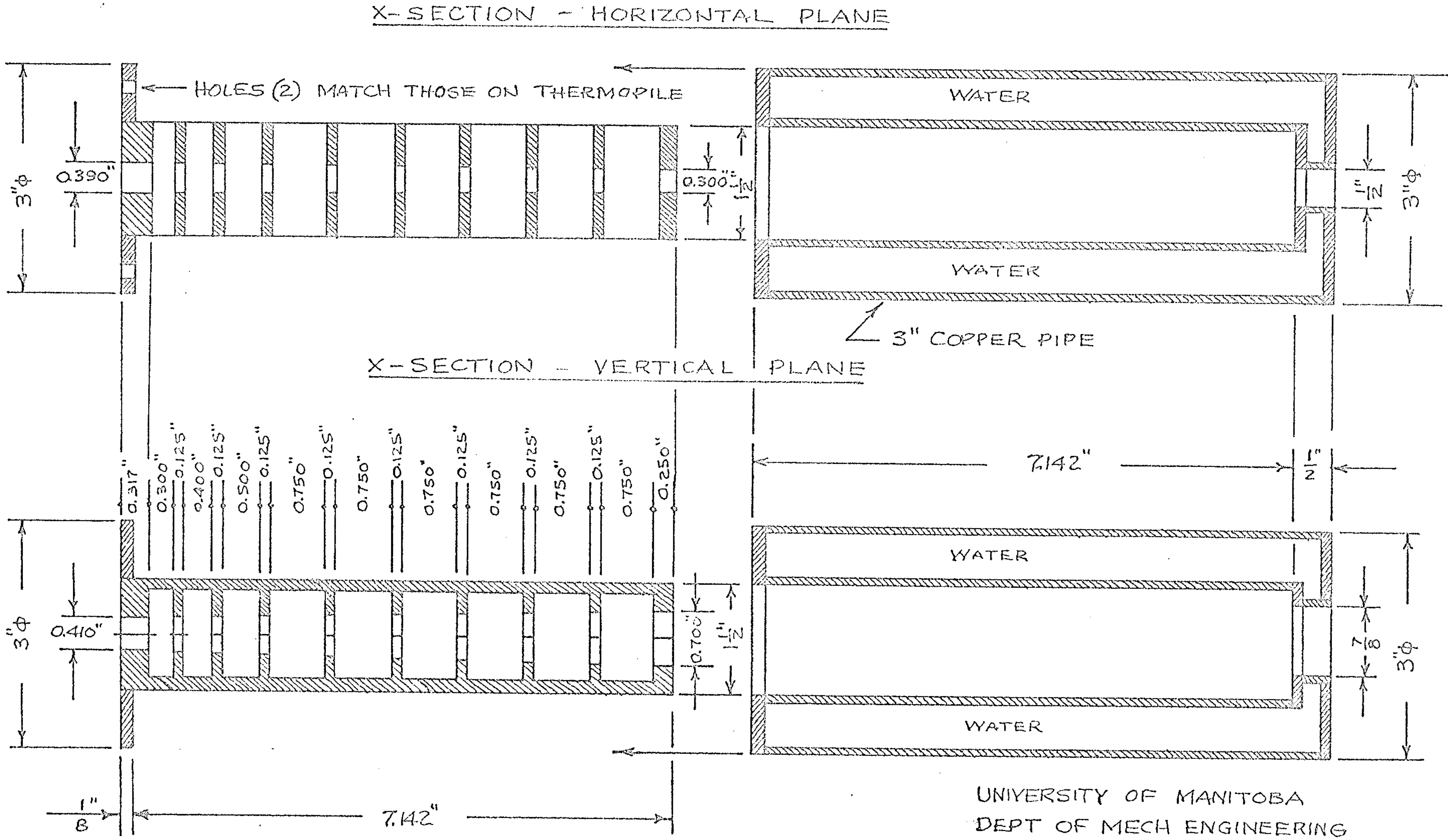

NOTE: ALL MATERIAL BRASS EXCEPT WHERE SPECIFIED

UNIVERSITY OF MANITOBA
DEPT OF MECH ENGINEERING
SCALE 1"=2" DATE JULY 22/63
DRWN HAH.

values. This sensitivity was measured with no window in place at a temperature of 22°C and 19% relative humidity. The amount of humidity in the air does make a sizable difference (estimated up to several percent) for a change of humidity from 20 to 60%. Since the relative humidity in the room remained constant throughout a test it would have negligible effect on the final results. A window made of CaF_2 was ordered with the thermopile but was not used in the tests.

Based on a shutter opening of 10.5 mm. the first diaphragm in the plane of the actual pile was set at 10 mm. (0.394 in.) square. By a series of full scale drawings to determine the sample size to be used, the front diaphragm size was set at 0.700 in. high and 0.300 in. wide. The space between the plane of the pile and the front diaphragm was set at 19.5 cm. (7.667 in.). The dimension of 7.267 in. shown in Figure 4 is 0.400 in. less than the set distance between front and back diaphragms because the actual plane of the pile is 0.400 back from the front face of the thermopile case. This is also the reason why the first diaphragm dimension is given as 0.390 in. by 0.410 in. high (i.e. the diaphragm size changes accordingly as you move away from the pile). The diaphragm assembly was machined from two pieces of solid brass $1\frac{1}{2}$ in. by $\frac{3}{4}$ in. cut to the required length of 7.267 in. After machining the diaphragm size lengthwise and removing the excess material between the diaphragms by machining crossways, the two pieces of brass were joined together by soldering to form a $1\frac{1}{2}$ in. square assembly with diaphragms of required size and spacing as shown in Figures 4 and 15. The diaphragms were painted with two coats of flat black paint on the sides facing the thermopile. The opposite sides of the diaphragms were polished to a dull shine.

This was done to minimize the effect of stray radiation reaching the thermopile. As well as this effect, the diaphragms tend to minimize convective currents inside the radiometer housing. The diaphragms are also positioned so that the thermopile cannot "see" the outside housing of the radiometer but only the diaphragms themselves.

The water cooled jacket covering the thermopile (Figure 15) was not used in the experiment because it was found that with the slight fluctuations in water temperatures which were experienced it was more beneficial to have this jacket removed. The other water cooled jacket over the diaphragm portion remained and was used in its original position. Since the water jacket of the thermopile was removed it became necessary to shield the thermopile from surrounding effects of radiation and convective currents. Aluminum foil was used as a shield with the polished side out. This shielding completely covered the thermopile and water jacket as shown in Figure 5. The entire radiometer assembly was pivoted about a $\frac{1}{2}$" shaft which protruded from the bottom of the thermopile case and was supported by an adjustable collar which made it possible to raise or lower the radiometer on the half circle metal table by which it was supported (See Figures 5 and 19). A spring loaded vertical pin at the collar allowed the radiometer to be located in three exact positions determined by three depressions drilled in the metal table at exact viewing locations. In this manner the radiometer could be turned to any of the three positions and as soon as the pin fell into place, the correct viewing position was attained. It was found that this particular arrangement worked very satisfactorily. The procedure followed in locating the three pin holes for viewing positions will be described

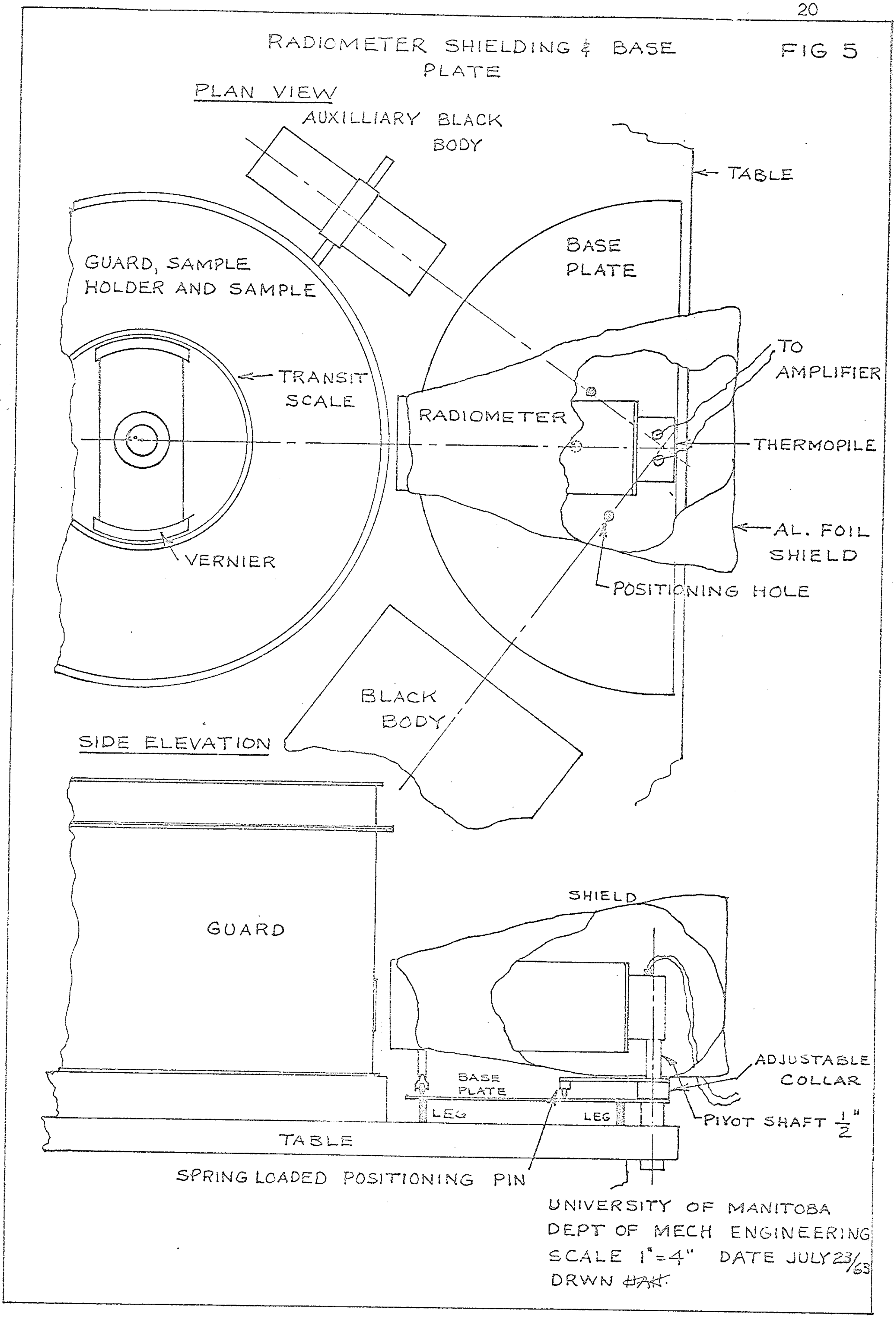
RADIOMETER SHIELDING & BASE PLATE
FIG 5
PLAN VIEW
AUXILLIARY BLACK BODY
TABLE
BASE PLATE
GUARD, SAMPLE HOLDER AND SAMPLE
TO AMPLIFIER
TRANSIT SCALE
RADIOMETER
THERMOPILE
AL. FOIL SHIELD
VERNIER
POSITIONING HOLE
BLACK BODY
SIDE ELEVATION
SHIELD
GUARD
ADJUSTABLE COLLAR
BASE PLATE
LEG
LEG
PIVOT SHAFT 1/2"
TABLE
SPRING LOADED POSITIONING PIN
UNIVERSITY OF MANITOBA
DEPT OF MECH ENGINEERING
SCALE 1"=4" DATE JULY 23/63
DRWN HAH

in a later section under apparatus assembling. Two thermocouples were placed to record water temperatures in the radiometer water jacket, one in the inlet flow line and one in the outlet flow line.

There was some drift in the zero position of the thermopile reading, but this was probably due to the fluctuation of the water temperature. Some zero drift could be tolerated because the readings were not taken for their absolute value but rather the difference was taken between a series of readings at the three viewing positions of the radiometer.

Black Body

No perfect black surface exists in nature and it is necessary to create one by artificial means. One of the easiest known methods is to build an isothermal cylinder with one closed end having the required length for the desired diameter and emissivity of the material. Buckley[7] did extensive investigations on radiation from an isothermal cylinder closed at one end. From curves shown in his work the value of the length required can be deduced so that the radiation shall be within 1% of full radiation. In this case, an l/r ratio of 6 was chosen. This meant, according to Buckley's curves,[7] that in order to obtain 99% of perfect radiation from the cylinder's open end it would be necessary to have a surface whose total hemispherical emissivity is approximately 0.48. It was felt that this could be accomplished by a copper oxide surface since emissivity values for copper oxidized surfaces go as high as 0.75 according to the literature. A copper cylinder was chosen with an internal radius of 1¼ in. By the l/r ratio of 6, this made the required length of the cylinder $7\frac{1}{2}$ inches. The closed end of the cylinder was covered with a $\frac{1}{2}$ in. copper plate of which a portion was machined out to obtain a very large angle cone effect. (Figure 6). The opening of the open end was cut down to $1\frac{1}{2}$ inches in diameter by placing a $\frac{1}{2}$ in. copper plate over it as well. The thickness of the copper cylinder was 0.083 in. It was therefore felt that by having the following, (1) the l/r ratio of 6 and emissivity of 0.48, (2) the large angle cone effect, and (3) the reduced size of the hole in the open end, that the desired 99% of perfect radiation could easily be attained.

Heat loss calculations were performed on this artificial black body assuming the temperature of the cylinder would be 1000°F maintained by a layer of insulation 2 in. thick with a thermal conductivity of 0.05 Btu/hr-ft-°F surrounding the cylinder. By this method it was concluded that a 250 watt heater would be sufficient. A 200 watt calrod heater would be sufficient. A 200 watt calrod heater was placed on the closed end of the heated cylinder. Two thermocouples were placed at the open end of the cylinder, two at the closed end and four more spaced evenly around the periphery between the open and closed end. (Figure 6 and 16). All these thermocouples were placed nearly flush with the inside surface of the cylinder. The black body cylinder was then placed inside a circular galvanized metal container 8 in. in diameter and 14 in. long. Thermocouples and power leads were taken out through the back of the container. (Figure 12). The space between the black body and the outer container was filled with a "Zonolite" brand "Vermiculite."

In order to attain a reasonably high value of emissivity on the inside of the black body, the cylinder was heated to approximately

CYLINDRICAL BLACK BODY FIG 6

X- SECTION

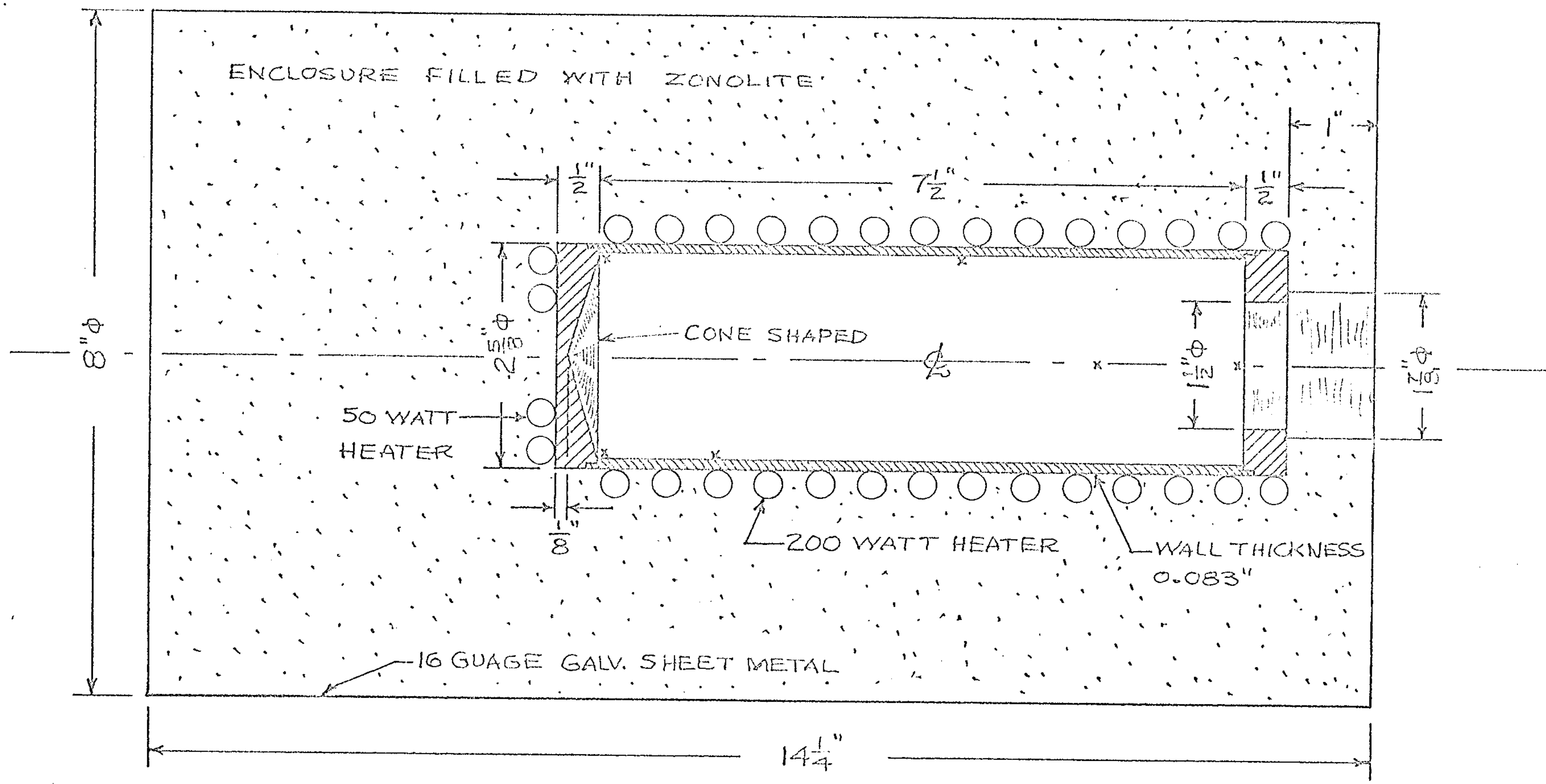

X – INDICATES THERMOCOUPLES

NOTE – THERMOCOUPLES AND POWER LEADS TAKEN OUT THROUGH HOLES IN BACK OF GALV. CONTAINER

UNIVERSITY OF MANITOBA
DEPT OF MECH ENGINEERING
SCALE 1" = 2" DATE JULY 22/63
DRWN ~~HAH~~

750°F and held there for about two hours after which the temperature was dropped to about 270°F and left at that setting. It was found that with the amount of insulation that was placed at the closed end of the cylinder that the end heater was not necessary. The temperature decreased towards the open end of the black body even when the end heater was turned off. It was therefore not used during any of the tests. All thermocouples worked satisfactorily except one. Even with this, a very good indication of the temperature distribution inside the black body was obtained.

To check the accuracy of the black body a sample of copper was tested after going through the same temperature sequence as the black body. The value obtained for the total normal emissivity was 0.45. This value was of course arrived at using the black body as it was, but even then the error could be assumed to be small. It was later noted as tests were performed that the readings obtained from the black body showed no appreciable change with time. The black body power supply to the main heater was continually left on. This was done to eliminate any unnecessary flaking of the oxide on the inside of the cylinder. The temperature at this setting was approximately 270°F (average). Four tests were run with the glass sample using a black body temperature of approximately 340° after which the temperature was returned to the previous 270°F setting. A change in readings of about 3% were noted on the black body after the higher temperature runs but this was not considered excessive because a certain amount of zero drift of the thermopile must also be accounted for. The temperature distribution inside the black body will be discussed in a later section under conclusions. Only two different temperatures were used in the black body because the type of analysis used on the data obtained did not require the black body temperature to be the same as the sample temperature at any time. Because of this it was not necessary to have a black body temperature control mechanism. An ordinary rheostat on a 115 volt power supply to the main heater was all the control that was necessary.

Sample Guard

In order to have a known and constant environment surronding the sample, a guard must be built which completely surrounds the sample at all times. To accomplish this, a concentric cylinder arrangement was used as shown in Figure 7 and 17. Two special cylinders of solid brass were made, one 14 in. in diameter and 7 in. high, the other 16 in. in diameter and 8 in. high. The lid was made separately as shown in the drawing. With this arrangement a 1 in. water jacket completely surrounded the inner space where the sample was suspended. Separate inlets were provided for cooling water to the lid and base of the guard container as well as outlets. The outlet water from the lid of the guard container went directly to the sewer but the outlet water from the base of the container was in turn passed through the auxilliary black body.

A small viewing hole $1\frac{1}{2}$ in. in diameter was drilled through the two cylinders to enable viewing of the sample when it was in position inside the guard. The whole inside of the guard was painted with three coats of flat black paint having tested normal emissivity of 0.95 and a hemispherical emissivity of 0.92. A small auxilliary black body was suspended from the outside of the guard container. This black body was

CYLINDRICAL GUARD ASSEMBLY

VERTICAL X-SECTION

FIG 7

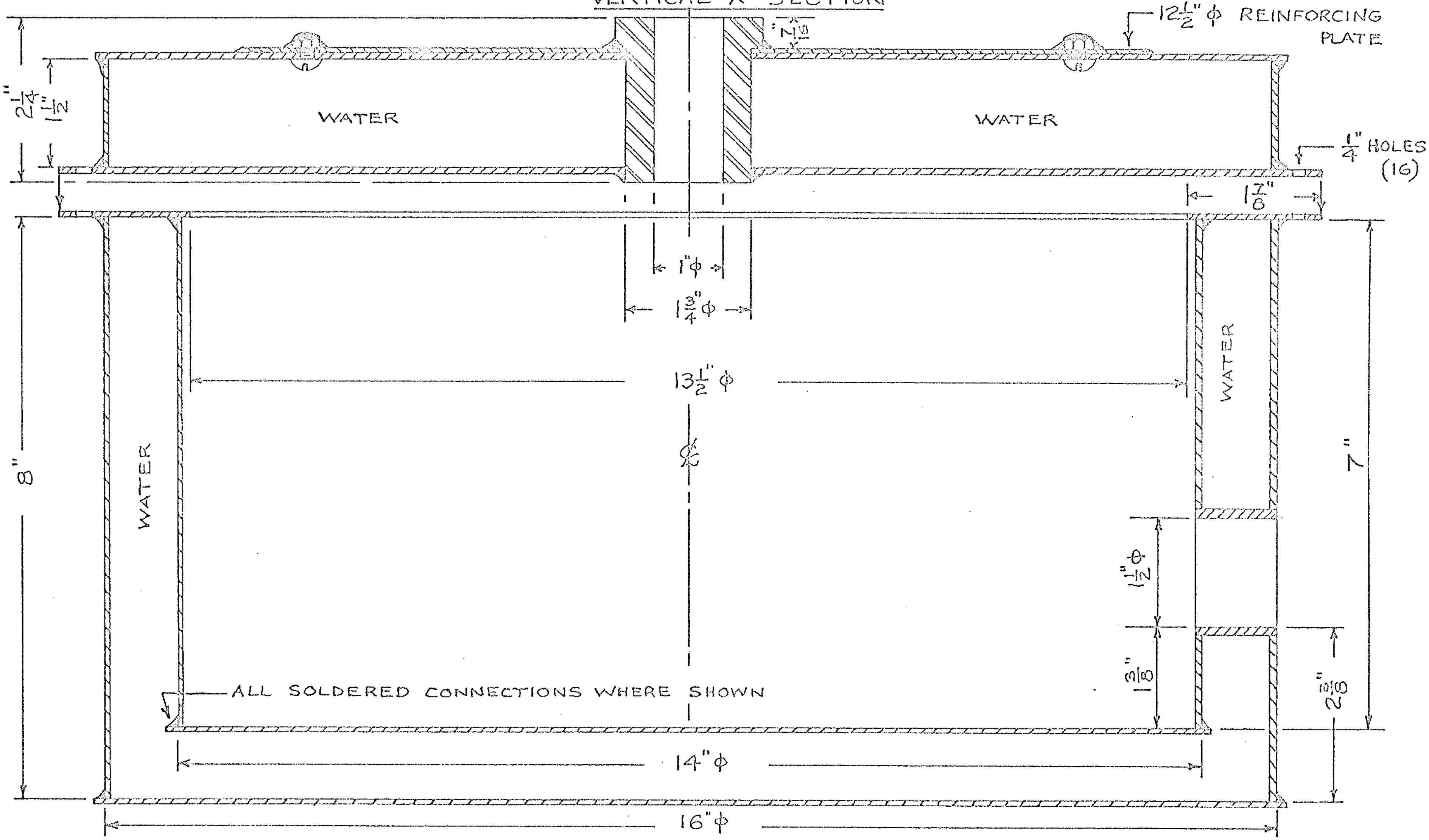

NOTE - TOP ASSEMBLY FOR ANGULAR MEASUREMENT SHOWN ON FIG

- ALL MATERIALS BRASS 1/16" THICK

UNIVERSITY OF MANITOBA
DEPT OF MECH. ENGINEERING
SCALE 1" = 2" DATE JULY 22/63
DRWN H.A.H.

composed of a $1\frac{1}{2}$ in. diameter tube $5\frac{1}{2}$ in. long surrounded by a 2 in. diameter copper tube 6 in. long. The space between the two cylinders was filled with water which had previously passed through the base portion of the guard container. In this manner the auxilliary black body assumed approximately the same temperature as the inside of the guard container (See Appendix C). The inside of the $1\frac{1}{2}$ in. diameter tube was painted with three coats of flat black paint to create a black body. Six thermocouples were inserted in the following positions, one in the inlet and outlet cooling water to the lid of the guard, two in the inlet and outlet cooling water supply to the base of the guard, and three in the inlet and outlet water supply to the auxilliary black body.

A surveyors transit scale was mounted on the lid of the guard and used to measure the required angle β from the normal to the sample. A full scale drawing of the set-up is shown in Figure 8. With the transit scale, the angle could be set to the nearest minute. By means of two set screws in the upper movable bushing, the sample holder could be raised or lowered to any desired position.

Sample Holder and Heater

As was mentioned previously, several scale drawings were used to decide the physical size of the sample, the critical dimensions of the radiometer, and the maximum angle that could be attained for measurement. A 13 in. long by 3 in. high sample area was a reasonably practical size. The length of the sample determined the inside dimension of the inner guard cylinder which was set at 14 in. diameter leaving a $\frac{1}{2}$ in. clearance dimension between the edges of the sample holder and the wall

ANGULAR MEASUREMENT ASSEMBLY FIG 8

VERTICAL X-SECTION

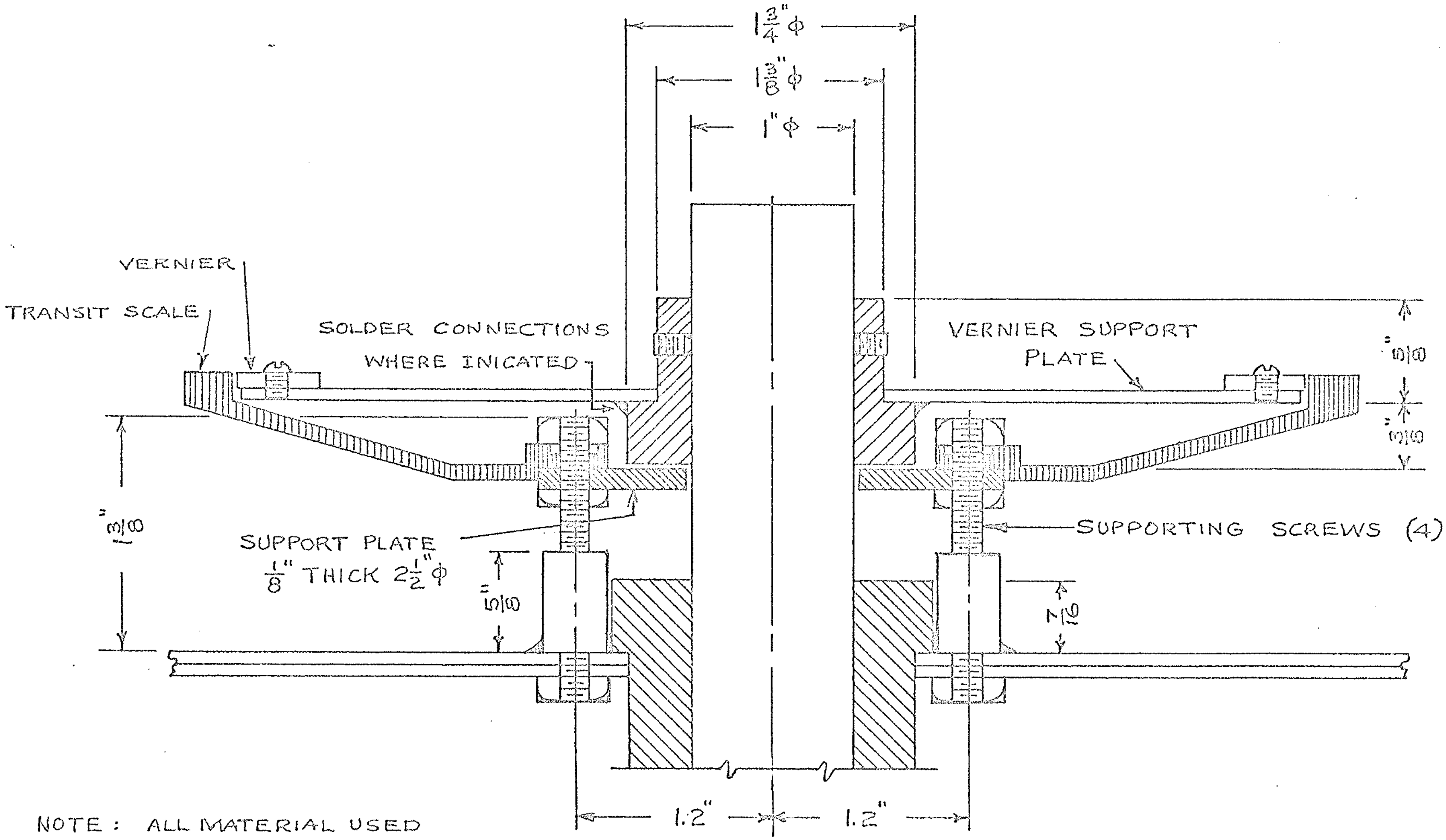

NOTE: ALL MATERIAL USED
IS BRASS

UNIVERSITY OF MANITOBA
DEPT OF MECH. ENGINEERING
SCALE: FULL SIZE DATE JULY 22/63
DRWN H.A.H.

of the guard container. With the radiometer dimensions set as previously described, the sample centre line position was set at about 16½ in. from the plane of the thermopile receiver. The maximum angle attainable was 83° according to the drawing. Thus all the critical dimensions of the sample holder, guard and radiometer were decided simultaneously.

A dimensional drawing of the sample holder appears in Figure 9. The main parts of the sample holder were made from aluminum. The sample holder was designed to take a sample as thick as ¼ in. with other dimensions of 13 in. by 3¼ in. high. Small flanges at the front of the holder accounte for a 1/8 in. overlap of the sample at the bottom and the top of the holder. This leaves an area of 13 in. by 3 in. high free to view by the radiometer. The brass bushing which is bolted immediately to the top of the sample holder was cut partially off at an angle so that the sample "sees" as little of this portion of the sample as possible. The aluminum flanges which overhang the sample surface were kept as thin as possible. The purpose of these implemented precautions is to keep the shape factor from the sample to the holder as small as possible thus keeping the shape factor from the sample to guard as large as possible. A small asbestos spacer was placed between the brass bushing and the 1 in. steel shaft to act as a barrier to heat conduction up the rod. It also insulates the sample holder from the guard container. When the sample holder and guard were assembled the maximum angle that could be obtained was 82.5°.

Heat loss calculations were carried out on the sample and holder using 1000°F as a maximum temperature. It was realized that at

SAMPLE HOLDER FIG 9

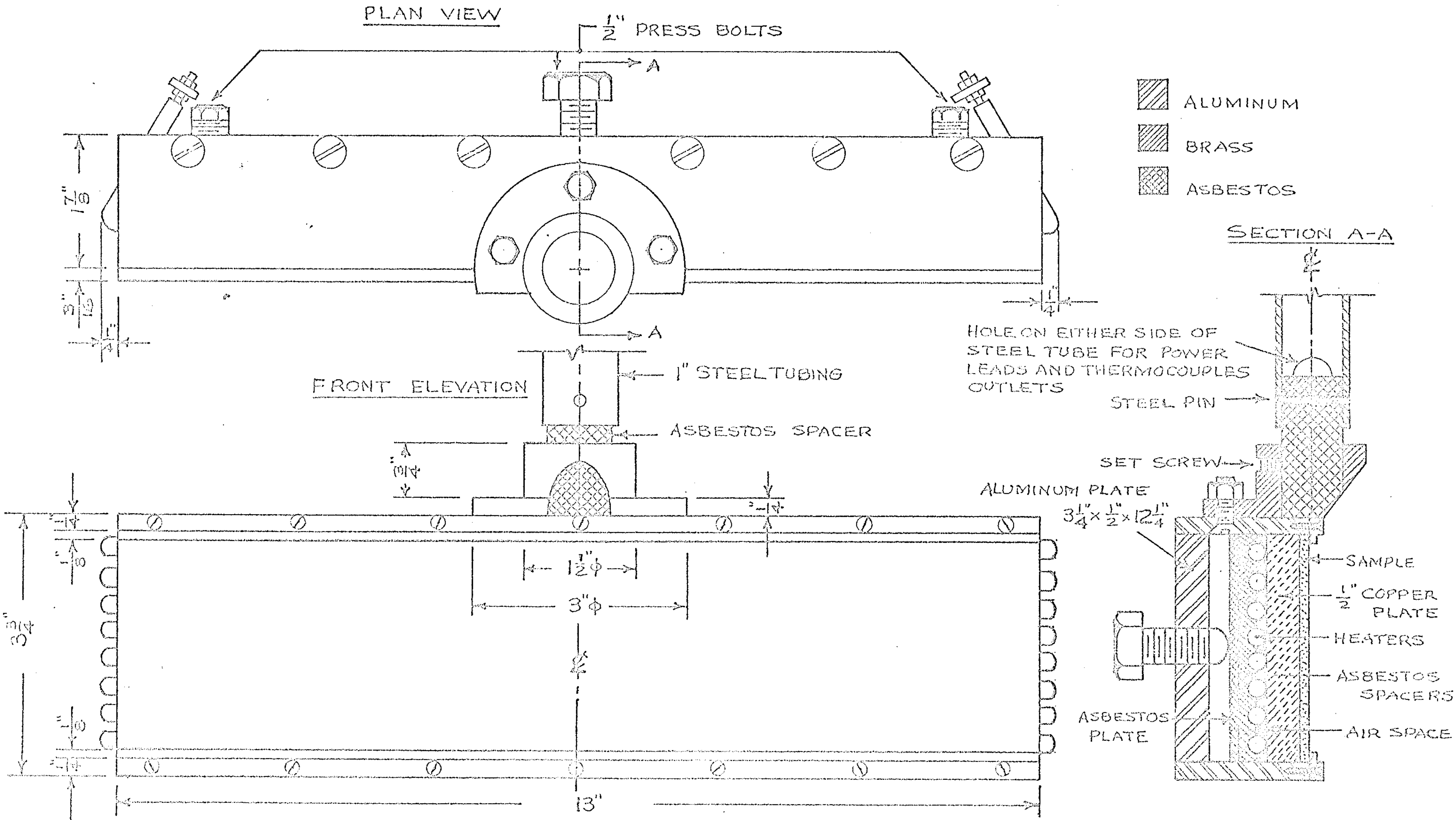

NOTE - SAMPLE HOLDER CONTAINS 8 HEATERS
AT 250 WATTS EACH

UNIVERSITY OF MANITOBA
DEPT OF MECH ENGINEERING

temperatures above 200°F or 300°F that the convective losses from the sample surface would be considerable but because the sample and holder were in a concentric container and the sample always remained in a vertical position, the convective losses would remain constant for any position chosen in a horizontal plane. Variations could exist for different vertical elevations on the sample. This could give rise to possible temperature variations in the plate surface. These variations were kept to a minimum since the vertical dimension was small in comparison to the length and second, all materials tested at high temperatures had high thermal conductivities and those with low thermal conductivities were tested at low temperatures. The glass results at high temperatures were not considered valid. There are some end effects but again these are very small. Also several thermocouples were placed in the sample to determine a good temperature distribution on the sample surface facing the radiometer.

In order to attain the 1000°F a heater of 2000 watts was used. The entire heater section was made of 8 calrod heaters of 250 watts each. They were bent as shown in Figure 10 and joined by two small bus bars at each end to form a single heating unit. The heater unit was placed directly behind the $\frac{1}{2}$ in. thick copper plate in the sample holder. Four small asbestos spacers were placed directly behind the heaters to keep them equally spaced in the holder and then another thin asbestos plate 13 in. long by $3\frac{1}{4}$ in. high was positioned behind the heater assembly. Three $\frac{1}{2}$ in. bolts in the back of the sample holder (Figure 9) were tightened in order to sandwich the entire assembly firmly against the flanges on the front of the sample holder. Since the heater length was $13\frac{1}{2}$ in. long at its widest point, this left only $\frac{1}{4}$ in. clearance between the heater edge and the wall of the guard. Placement of the heater was critical because any small amount of excess overhang would cause the heater to rub along the guard wall.

The thermocouples and power leads were brought out of the inside of the guard by running them inside the one inch steel pipe which supports the sample holder. The power supply used was 115 volts controlled by a variac. After several tries on the power setting of the variac, it was relatively simple to obtain a desired temperature within a small range.

<u>Cooling Water Supply</u>

Water from the hot and cold water lines was proportioned to obtain cooling water at room temperature. Extreme fluctuations of water temperature during the daytime hours necessitated running all the tests at night. Even then fluctuations of several degrees were noted. To even out these fluctuations as much as possible the water was passed through a radiator and finned tube in series after which it flowed to a head tank. A line from the head tank fed the apparatus with cooling water. (Figure 14). Any temperature fluctuations which remained had to be tolerated.

The flow of water through the apparatus was controlled by three cocks on the outlet side. Since there was no excessive heat pickup in the apparatus, flows were moderate but high enough to maintain a reasonably high convective heat transfer coefficient on the water side of the guard container. To measure the water temperature, special thermocouple wells were machined from brass. The wall thickness was approximately 0.008 to 0.010 in. thick. Each well was filled with oil into which the thermocouple was inserted and held in place by a cork.

Measuring Equipment

Two main instruments used for measuing means in this experiment were (1) a stabilised D-C microvolt amplifier and (2) a portable precision potentiometer. Both instruments were made by Leeds and Northrup.

For the D-C amplifier the limits of error given by the manufacturer are:-

(a) of amplifier response: ± 0.4% of range span,

(b) of meter reading: add 1% to (a),

(c) of zero: maximum of set ± 0.5 microvolts within which drift will not exceed 0.2 microvolts during a 1 minute interval, after warm up. The amplifier has a response time of two seconds for 2000 ohms maximum source resistance and three seconds for 10,000 ohms maximum source resistance. These are approximate values for the instrument to obtain within 1% of balance. The amplifier has the following ranges with corresponding magnification factors as tabulated;

Range	Magnification Factor
0 to 50 μv	200
0 to 100 μv	100
0 to 200 μv	50
0 to 500 μv	20
0 to 1000 μv	10
0 to 2000 μv	5

The maximum output on all ranges is 10 millivolts.

The accuracy of the amplifier was checked before any of the tests were performed. Two potentiometers were used accurate to $\pm$ 0.005 mv. One potentiometer was used to apply a biased emf input to the amplifier and the other used to measure the output from the amplifier. The potentiometers were also interchanged and the same procedure carried out. It was proven by this method that the error in the amplifier was well within the limits stated by the manufacturer.

The potentiometer is designed primarily for measurement of thermocouple emf's but may be used to check other potentiometers. The instrument has two ranges, one of 0 to 16 millivolts and one of 0 to 80 millivolts. On the low range it is possible to read to the nearest 0.01 of a millivolt and estimate the third decimal if necessary. On the high range, you may estimate the second decimal point but no further.

Miscellaneous Equipment

(1) A twenty-eight position thermocouple switch and thermocouple wire.

All thermocouples were made of # 24 guage iron constantan wire. In the preparation of each junction, a 40 volt A.C. voltage source was used. One lead from the source was connected to the thermocouple wire. The other lead was connected to a small copper terminal which extended into an ink bottle half filled with mercury covered with a thin film of light transformer oil. To form a thermocouple bead, the twisted end of the thermocouple wire was dipped momentarily into the mercury at which time an arc occured. Each bead thus formed was tested for continuity and observed under a microscope for any irregularities.

The accepted accuracy value as published for the iron constantan wire was ± 0.5%. This was checked at 32°F and 212°F and found to be within ± 0.25% or within the limits of the potentiometer.

Twenty three couples were originally hooked up. Two of these were not used since they read the inlet and outlet water temperature to the thermopile cooling jacket which was discarded before measurements began. One of the thermocouples in the black body read incorrectly and was disregarded.

The thermocouple selector switch used was made by Lewis Eng. Co., Type 27 S 38 B4 (Serial No. 3361). The positioning of the switch and various couples may be observed in Figure 28 (Appendix A).

(2) An ordinary thermos for cold junction reference of thermocouples. Two leads entered the reference flask. Exterior copper leads to the potentiometer were connected at a common location to the thermocouple leads. No thermal gradient existed near or at the junction point.

(3) Two power variacs to controller heater power supply.

A 1.6 KVA (115 volt) variac was used to regulate the power supply to the main heater of the black body. A 2.0 KVA (115 volt) variac was used to regulate power to the sample heater.

SAMPLE HEATER ASSEMBLY FIG 10

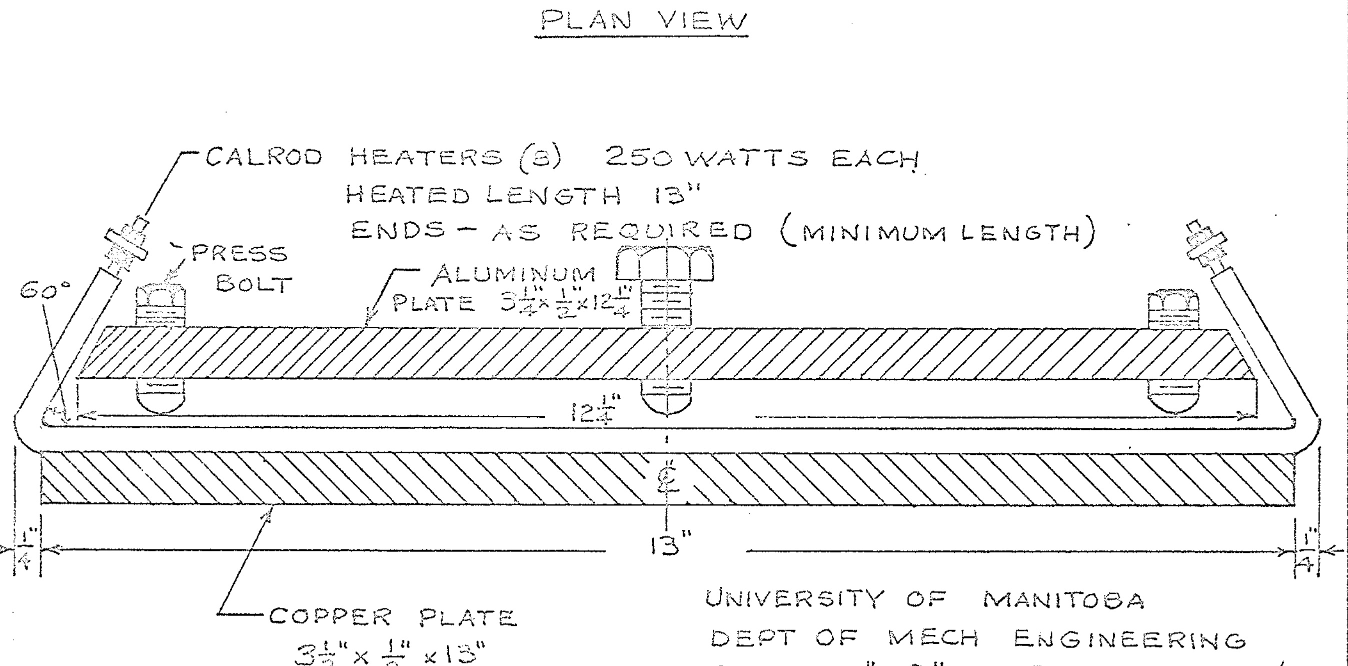

UNIVERSITY OF MANITOBA
DEPT OF MECH ENGINEERING
SCALE 1" = 2" DATE JULY 22/63
DRWN HAH.

THERMOCOUPLE LOCATIONS ON SAMPLES FIG 11

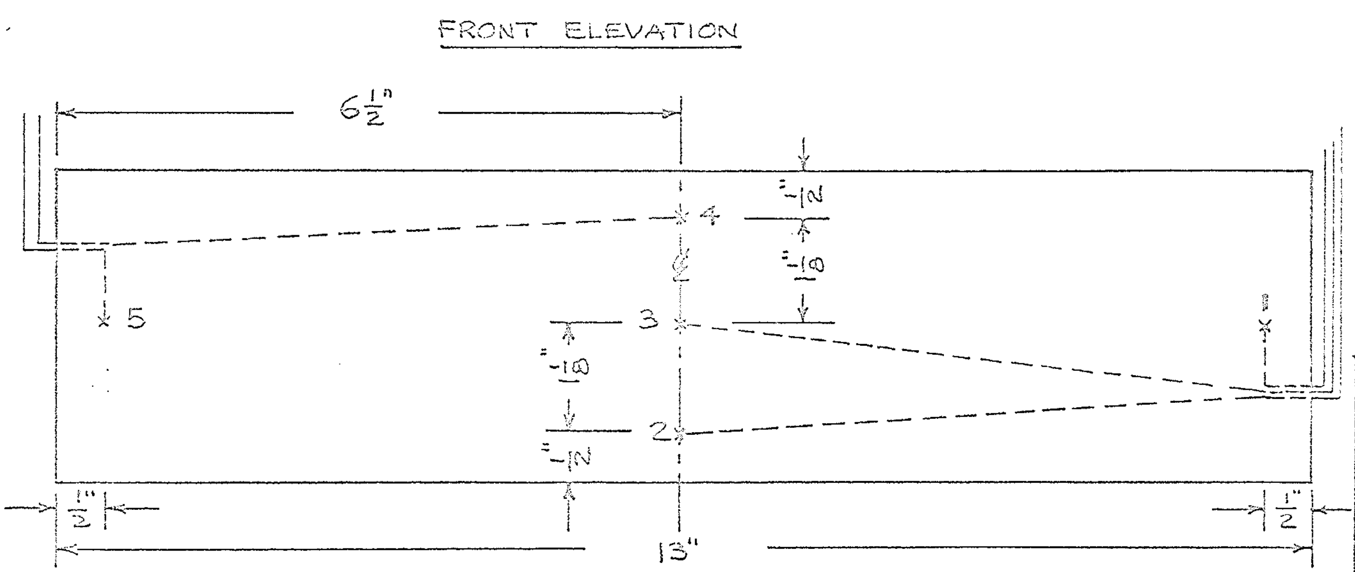

UNIVERSITY OF MANITOBA
DEPT OF MECH ENGINEERING
SCALE 1" = 2" DATE JULY 22/63
DRWN HAH.

V SAMPLE PREPARATION

Five different samples were tested for their directional emissive properties. These were copper, aluminum, aluminum foil, glass and painted copper, in that order. Thermocouples were placed on each sample and the surface cleaned of any foreign matter.

Copper Sample

A 1/8 in. thick plate of pure copper was cut to sample size, 13 in. long by $3\frac{1}{4}$ in. high. Grooves 0.080 in. deep were machined in various positions as shown in Figure 11. Holes were drilled to within 0.010 in. of the front surface in each of the five positions indicated. The thermocouple beads were placed in the holes and cemented into place with thermon. The remainder of the thermocouple wire was laid in the milled groove and led to the outside edge of the plate.

Excess thermon was removed from the back of the plate and the sample was placed in position in the sample holder. Three series of emery cloths were used to smooth the surface as much as possible. The emery cloth was Struers pregrinder grits 320, 400 and 600. The operation was done by hand. Finally, the sample surface was cleaned with acetone to remove any dirt and finger prints. The sample was then located in place and tested.

Aluminum Sample

Exactly the same procedure was followed in preparing the aluminum sample.

Aluminum Foil Sample

Since the aluminum foil was too thin to use alone it was placed on another surface. It was decided that since the copper plate had a very high thermal conductivity, it would be the best material to use. The same copper plate was used as described previously. A thin layer of varnish was applied to the front surface of the copper plate. The aluminum foil was then rolled on and the excess trimmed from the edges. The initial thermocouples were replaced with new ones in the same manner as described in part A. Since there was 0.010 in. of copper, a very thin layer of varnish and a thin layer of aluminum foil in series, it was assumed that the thermocouples would give a good indication of the surface temperature of the aluminum foil. The surface was cleaned with acetone and the sample put into place and tested. Care was taken during the entire process so as not to scratch or mar the surface of the foil.

Glass Sample

Unlike the majority of solid materials, glass is transparent to certain radiation wavelengths. It is nearly opaque to radiation wavelengths beyond approximately 3μ and transparent to radiation at shorter wavelength. All wavelengths of radiation are given off by the surface which is directly behind the glass plate. Hence, some of the radiation reaching the receiver comes from the metal which is directly behind and in contact with the glass. The total radiation reaching the thermopile is given by the equation:

$$R = R_g + R_m \gamma_g$$

where R_g is the radiation from the glass, R_m that which would be received from the metal if the glass were not present, and τ_g the transmittance of the glass for this radiation.(8) The transmittance τ_g can be calculated if the spectral distribution of R_m is known and spectral-transmittance data for the glass is available. The spectral transmittance is dependent on the thickness of the glass and the type of glass under test. The exact data were not available for the glass used. It was decided to run the tests and neglect the second term on the right hand side of the above equation and compare the results with existing data to ascertain the validity of the assumption.

The glass sample was cut to the same dimensions as the other samples. The thickness was approximately 1/8 in. Thermocouples could not be positioned as they were in the other samples because of the difficulty in machining or drilling glass. Therefore, the thermocouples were placed on the front surface of the glass by cementing them into place with thermon. A thermocouple was not placed in position # 3 as shown in Figure 11. The wires for thermocouples # 2 and # 4 were run very close to the bottom and top edges of the sample respectively so they would not be "seen" by the radiometer during testing. Extreme care was taken to have the thermocouple beads touching the glass surface so as to obtain as true a surface temperature as possible. By running the thermocouple leads along the sample, the couples tend to attain temperature equilibrium with the glass plate. Thermocouples were surrounded by thermon which has a thermal conductivity approximately that of iron. The thermon tends to assume the same temperature as the glass surface. The error was assumed to be negligibe or small at low temperature. More explanation on actual values is given in the results.

Painted Copper Sample

The same copper plate was used as previously described. The holes where thermocouples were placed were extended to just break the surface of the copper. The thermocouples were positioned as previously described under the copper sample.

After the thermocouples were placed, the front surface was painted with three coats of flat black paint made by Northern Paint Co. The sample was positioned in the holder and tested.

VI APPARATUS ASSEMBLING

Figure 3 shows the approximate locations of all components of the apparatus. The guard, radiometer, black body, one variac, thermocouple switch and ice bath were placed on a rigid table. The remaining variac and two instruments were placed on a counter next to the table in the room. Before the tests could be performed the radiometer, black body and guard were placed in exact alignment with one another. The procedure followed is listed below:

1. The table upon which the apparatus was to be placed was leveled.

2. The base plate holding the radiometer was positioned and leveled close to one edge of the table. This assured that the radiometer pivot shaft was vertical.

3. Before the sample holder and sample were placed inside the guard container, the vertical centre line and horizontal centre line of the sample were identified on the sample surface. A small circular mirror was placed over the centre point of the sample and taped in place. The thermocouples and power leads from the sample and sample heater respectively, were brought out through the 1 in. steel shaft. The sample holder was now placed in the guard container and the lid was secured.

4. A line passing through the centre of the guard had been marked on the bottom of the guard when the $1\frac{1}{2}$ in. viewing hole was drilled previously. This same line was used to align the radiometer with the guard assembly. (i.e. the centre line of the radiometer was made to

coincide with this line). The guard was placed on two boards which raised it about $1\frac{1}{2}$ in. above table level. The guard was moved forward until the radiometer, when rotated, cleared the viewing hole in the guard by about $\frac{1}{4}$ in. The guard assembly was leveled in this position and secured to the table.

5. The back of the thermopile was removed and a light source was placed inside the guard so the mirror was visible. By looking through the back of the radiometer one was now able to "see" the sample. First, the sample holders vertical position was set by adjusting the set screws in the bushing on top of the guard. The sample holder position was set so that approximately $\frac{1}{4}$ in. space remained between the bottom of the holder and the bottom of the inside guard container. The vertical position of the radiometer was then set to make the horizontal centre line of the thermopile correspond with the horizontal centre line of the sample surface.

6. By looking through the back of the radiometer and rotating the sample holder and radiometer slightly, one was able to "see" the image of the front diaphragm of the radiometer in the mirror. When the image of the diaphragm appeared to be reflected straight back, the radiometer centre line was taken to be exactly perpendicular to sample surface in both the vertical and horizontal plane.

7. With the sample holder in the above position the verniers were adjusted to read zero on the transit scale. Also a mark was made on the base plate of the radiometer where the spring loaded pin fell. A small depression was then drilled in the base plate. By positioning the sample using the transit scale setting and radiometer with the spring

loaded pin, the perpendicularity was again checked as above and any minor adjustments made if necessary. It was found that the spring loaded pin positioner on the radiometer worked very well, always stopping the radiometer in the same exact position. Once the radiometer position was set and the verniers of the transit scale read correctly the maximum angle that could be turned was determined. While looking through the back of the radiometer towards the sample, (with light source in place inside the guard) the sample was rotated slowly and stopped in a position where the outer edge of the sample first became visible. The reading on the transit scale at this point was 82.5°. Thus, it was surmised that 82° would be the maximum angle used in the actual test.

8. The auxilliary black body had been mounted on the side of the guard with its opening at the same level as the viewing hole of the guard. It was therefore only necessary to align the centre line of the radiometer. This positioning was not as critical as the previous. When the two were in line, a second depression was drilled in the base plate of the radiometer for the radiometer positioning pin.

9. The radiometer was again rotated to view the large black body. The black body centre line and radiometer centre line were aligned. The black body was positioned vertically so that the radiometer viewed the black body through the centre of its opening. When this was established a third depression was drilled in the base plate to yield the final hole for the positioning pin. Thus the three exact viewing positions of the radiometer had been determined.

10. All thermocouples and power leads were connected. The thermopile output was connected to the D.C. amplifier and the amplifier was grounded. A double pole, double throw switch was used in conjunction with the potentiometer to enable readings to be taken from either the thermocouples or the thermopile.

11. All water supply and return lines were connected.

12. After some preliminary tests were run, it was found necessary to connect the radiator and finned tube to the water supply in an attempt to reduce the magnitude of the water temperature fluctuations. The radiometer was shielded with aluminum foil after it was determined that the water cooled jacket on the thermopile was not beneficial.

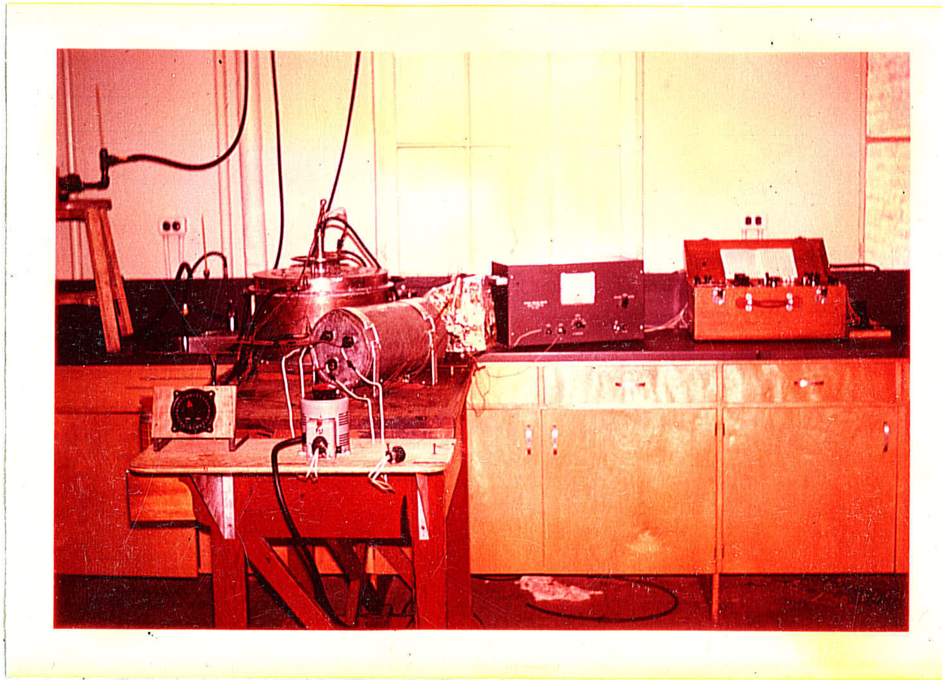

Figure 12

GENERAL ARRANGEMENT - A

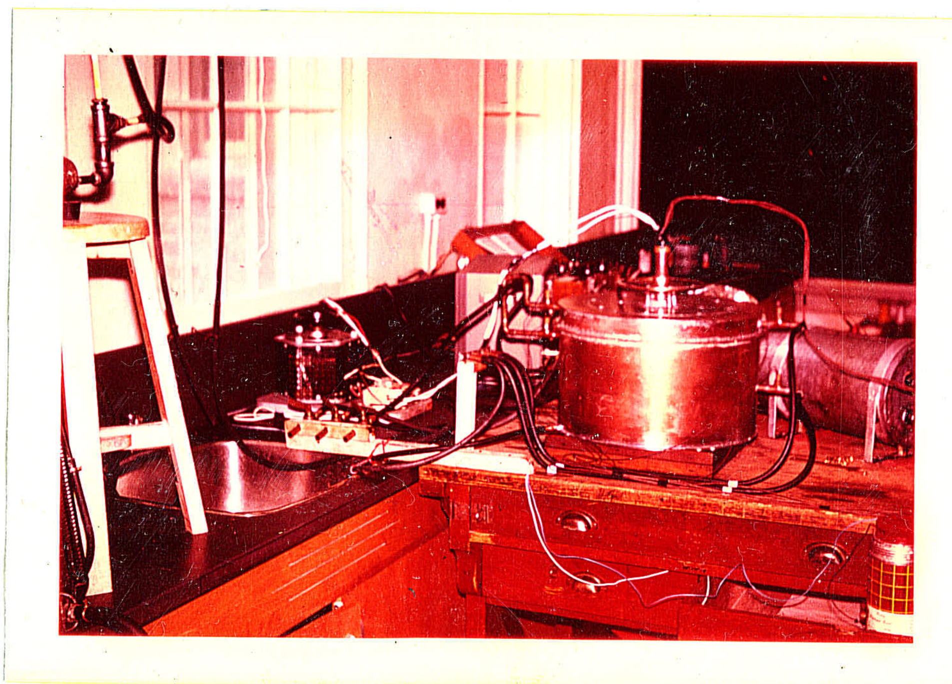

Figure 13

GENERAL ARRANGEMENT - B

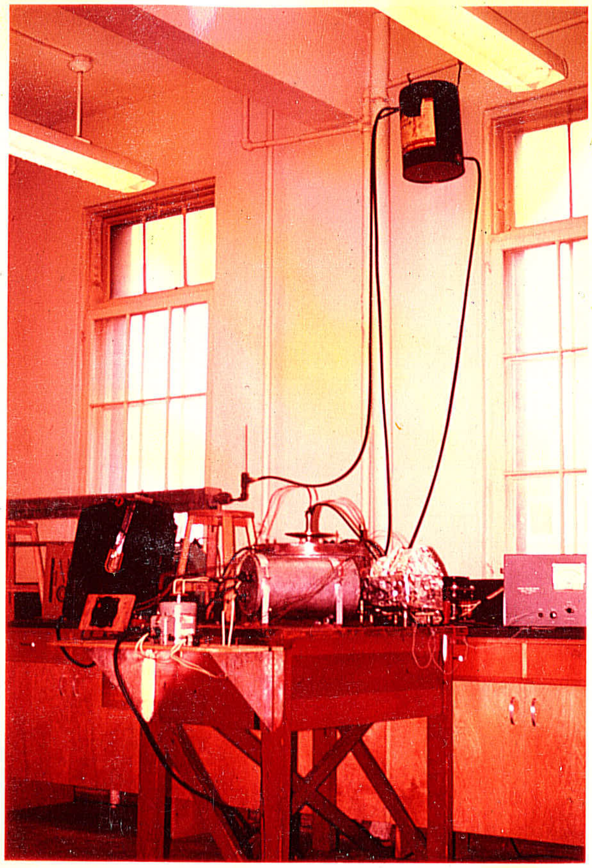

Figure 14

GENERAL ARRANGEMENT - C

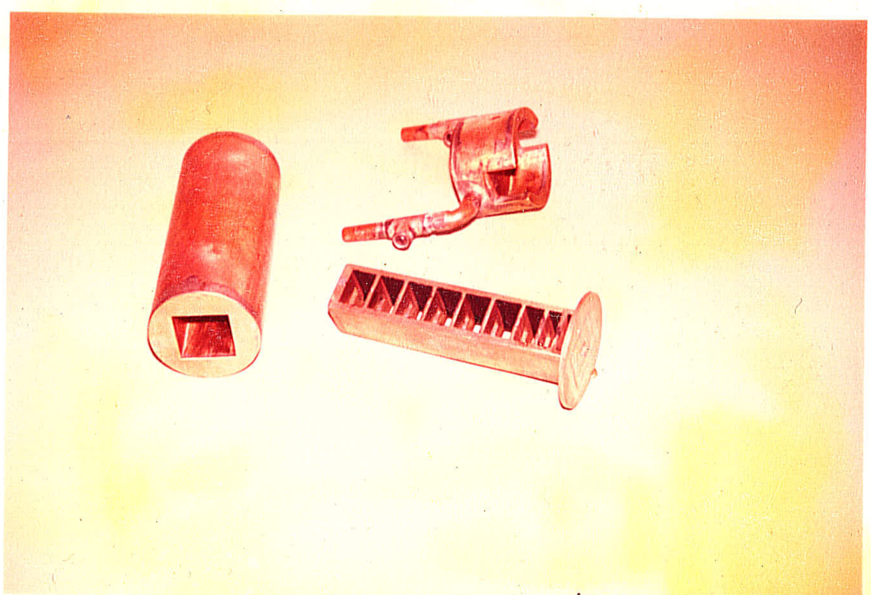

Figure 15

RADIOMETER - NOT ASSEMBLED.

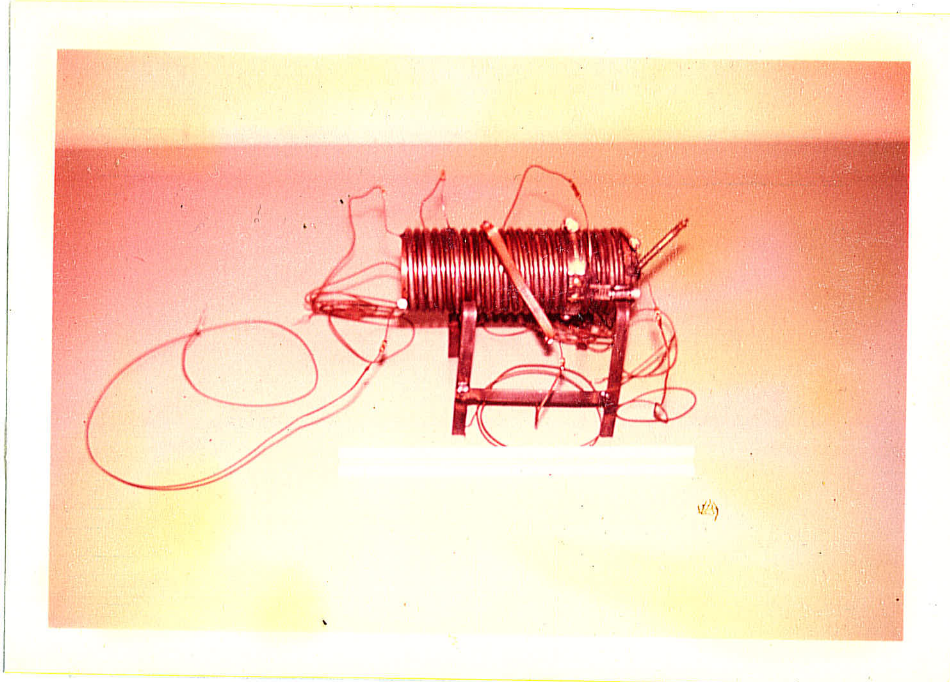

Figure 16

BLACK BODY - SHOWING THERMOCOUPLES

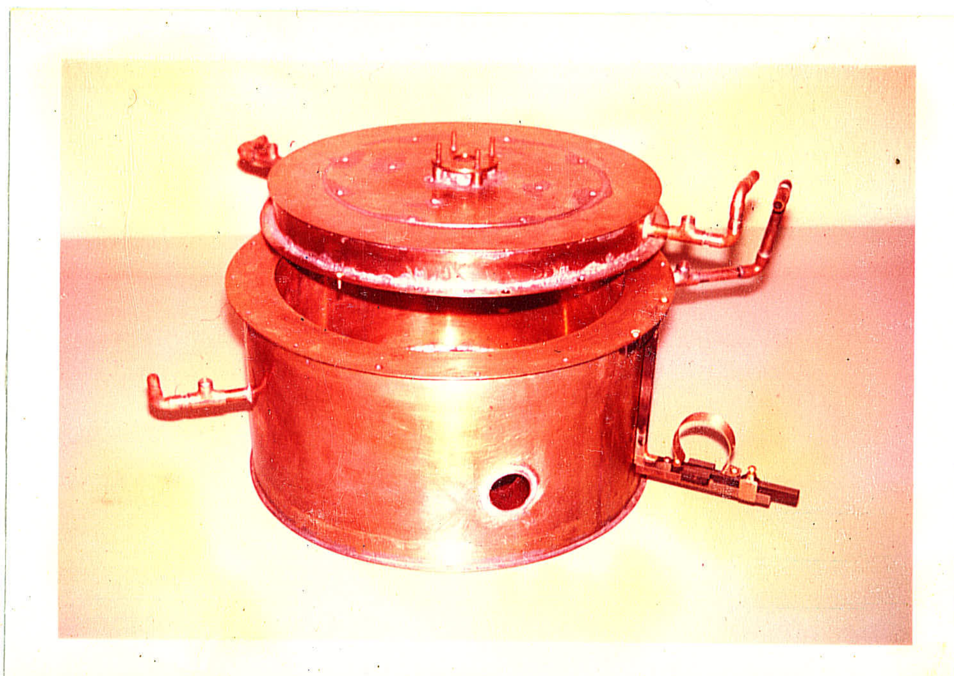

Figure 17

GUARD ASSEMBLY

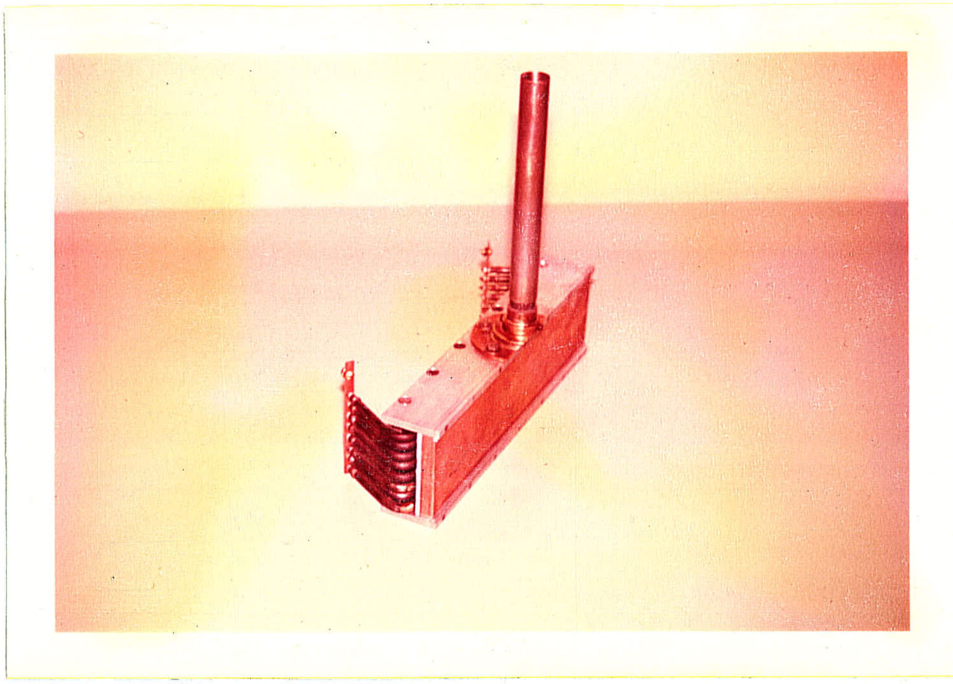

Figure 18

SAMPLE HOLDER

Figure 19

PLAN VIEW OF RADIOMETER

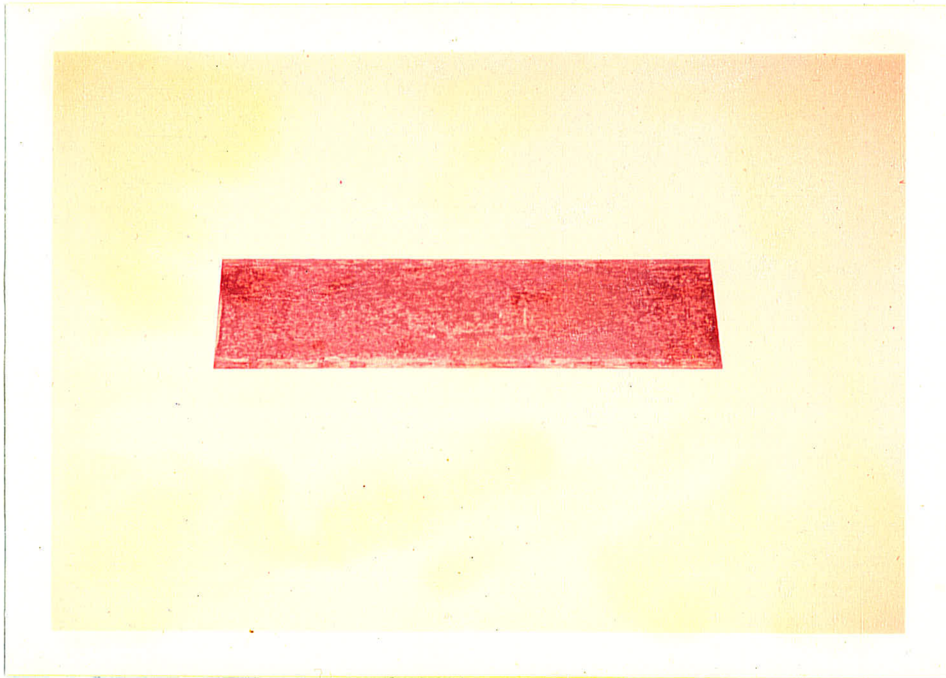

Figure 20
COPPER PLATE

VII TEST PROCEDURE

Once the three positioning holes were determined for the radiometer the test procedure became relatively simple.

1. The cooling water was turned on and the portions of hot and cold water were adjusted to yield a water supply at room temperature. The various flow rates were set so that there was just a small trickle of water from the overflow on the head tank.

2. The power was turned on for the sample heater and the variac was set at the desired voltage. The black body was left on continually.

3. The ice was placed in the thermos and the cold reference junction was inserted. Both instruments were turned on and adjusted for zero position. The apparatus was allowed to reach equilibrium conditions whereupon the test was begun.

4. Emf's for all the thermocouples were taken with the time being noted.

5. The radiometer was rotated from position to position with readings being taken in the following order:

   (a) Auxilliary black body,

   (b) Sample,

   (c) Main black body,

   (d) Auxilliary black body,

   (e) Sample.

This procedure was repeated for the following angles, 0°, 10°, 20°, 30°, 40°, 50°, 60°, 65°, 70°, 75°, 80°, 82° and back to 0°. Step (c) was only performed at 0°, 30°, 60° and 82° since it remained reasonably constant throughout the test. The time was noted for each set of readings taken, for each angle. Occasionally, the time was only taken at intervals when the test had to be discontinued momentarily to wait for water temperature fluctuations to dissipate.

6. When the readings on the radiometer were completed all thermocouple emf's were again taken with the time being noted.

7. To complete the test, the wet and dry bulb temperatures were taken.

The data sheet is shown in the sample calculation section (Appendix B). Thermocouple emf's were averaged and the corresponding temperatures found from the appropriate tables.

VIII RESULTS

Five samples were tested, two non-electrical conducting, materials and three electrical conductors. Each sample was tested over approximately, the same temperature range, 200°F to 800°F, to attempt to establish any trends in the change of emissivity with temperature. The directional emissivity and total hemispherical emissivity were calculated for each sample. The directional emissivities are tabulated as designated in the following subsections. The total hemispherical emissivity for each sample and the ratio of the total hemispherical emissivity to the total normal emissivity appear in Table 5.

Copper

Some difficulty arises in testing a material such as copper over the design temperature range because of the changing characteristics of the surface as the sample is heated to various temperature levels. The sample was polished to as smooth a surface as possible with fine emery cloth before the tests were begun. The polishing was done in the horizontal direction with respect to the test position. None or very few vertical scratches or discontinuities remained in the vertical direction. Tests # 1 to # 7 inclusive were run on the copper sample at temperatures indicated in Table 1. Once the maximum temperature test was performed there were no extreme changes in emissivity values on the following two tests, # 6 and # 7.

Directional plots for Tests # 1 and # 5 appear in Figures 22 and 23 respectively. It may be noted from Figure 23 and the results of

Test # 6 and # 7, that both conductor and non-conductor properties are shown. This fact may be born out by Figure 20 which is a photo of the copper plate after it was removed from the apparatus. An oxide coating appeared on the surface but it was not uniform and had scaled off in numerous positions. This double property relationship is also shown by plotting the obtained values of ϵ_H/ϵ_N on Figure 2. The value falls between the theoretical plots[3] for conductors and non-conductors. The ϵ_H/ϵ_N value for Test # 1 is slightly higher, which it should be, for the oxide layer had only started to form at this low temperature and the metallic properties prevail.

As may be seen from the results of Tests # 2, # 3 and # 4, the surface conditions of the plate changed as the temperature was increased. It is difficult, for copper, to compare results with published values because of the different degrees of oxidation which may be obtained on such a sample. McAdams[4] gives a total normal emissivity for a copper plate oxidized at 1110°F as 0.57 for a temperature range of 390°F to 1110°F. This is considerably different from our value of $\epsilon_N = 0.45$ but a temperature of 1110°F was not attained in the tests and this would probably account for the difference.

To check the validity of Equation (10) by Schmidt and Eckert[3], a value of ϵ_N was calculated at 202°F for the copper sample. The value obtained was $\epsilon_N = 0.0155$. This total normal emissivity was considerably lower than any results obtained by measurement in these tests and also lower than the lowest published value of $\epsilon_N = 0.030$[3] for a highly polished copper plate.

Aluminum

The formation of any additional oxide on the surface of the aluminum was virtually undetectable in the results of the tests or by visible inspection of the plate after it was removed at the completion of the tests. The sample was originally polished in the same manner as the copper sample. Tests # 8 to # 14 inclusive were run at the temperatures given in Table 2.

There is a noticeable increase in the emissivity values for Tests # 10, #11, and # 12. Each test shows the same increase over the previous. The increase was not attributed to the formation of an additional oxide coating because for Tests # 13 and # 14 the emissivity values decrease again to produce results even slightly lower than the first two low temperature runs, Tests # 8 and # 9. This change may have been due to a surface condition change in the aluminum caused by the annealing of the sample at the high temperature. The increase in emissivities with an increase in temperature is a common characteristic of metallic surfaces. A directional plot for Test # 10 is given in Figure 24.

The hemispherical emissivities and ϵ_H / ϵ_N ratios are listed in Table 5. Except for the ϵ_H / ϵ_N values for Tests # 8 and # 9, the remaining values show definite conductor properties. For an aluminum surface oxidized at a temperature of 1110°F, McAdams[4] gives values of ϵ_N as 0.11 to 0.19 for a temperature range of 390°F to 1110°F. The total normal emissivity values of our tests fall well within this range. Aluminum has the property of oxidizing very quickly and then showing very little change with age or increase in temperature.

Equation (10) was used to check the total normal emissivity of aluminum. The value calculated for a temperature of 202°F was $\epsilon_N = 0.0212$. This value is again lower than any of the results obtained and lower than the published result [(3)] values at that temperature.

Aluminum Foil

Only four tests were run on the aluminum foil because the equipment, up to this point, seemed to be performing quite reliably. Temperature and emissivity values are recorded in Table 3. There is an unaccountable drop in the emissivity values of Tests # 15 and # 16. It was first thought this drop was due to incorrect temperature readings caused by the aluminum foil breaking the bond between itself and the copper plate. This may have been partially responsible, for when the sample was removed, there were areas where the aluminum foil had formed very thin air pockets. These pockets did not appear directly in front of any of the five thermocouples and the temperatures at these positions were assumed to be correct but it may not have been the same in positions where air pockets existed. This situation may have resulted in temperature gradients existing on the sample surface which would become more pronounced at higher sample temperatures. The two low temperature runs yield similar values. These values are very close to those obtained by Schmidt and Eckert[(3)] as indicated in Table 3.

It was mentioned previously that for bright metallic surfaces that the total hemispherical emissivity was usually 1.15 to 1.20 times the total normal emissivity.[(3)] This is born out by the values of

ϵ_H/ϵ_N in Tests # 16, # 17 and # 18. Test # 15 is slightly low but one must keep in mind that any small change in the value of ϵ_N would change the ratio considerably. By comparing both the directional and total hemispherical emissivities with published results, it is concluded that the results of Tests # 15 and # 18 are most reliable. A directional plot for Test # 15 is shown in Figure 25.

Glass

As tests were run at higher temperatures, it became evident that either some radiation was passing through the glass from the copper plate or the thermocouples were not giving a true temperature. One of the four thermocouples gave an extemely low emf compared to the others so this low temperature reading was not included in the calculations. The remaining three were in good agreement on temperatures below 300°F.

It was confirmed that the assumption made previously on neglecting the radiation passing through the glass was false at high temperatures but not for temperatures below 300°F. It was mentioned previously that no radiation having a wavelength of greater than 3μ will pass through the glass. Assuming the plate behind the glass emits black radiation at a temperature of 340°F, the portion of radiation emitted below a wavelength of 3μ is approximately 0.5% which introduces negligible error compared to others. Errors in surface temperature measurement plus others are inherent in all test results. Because of these reasons, results of Tests # 19, # 23, # 24 and # 25 are included as good continuity exists. Tests # 20, #21 and # 22 were believed to include excessive errors and therefore excluded. Tests # 19, # 23 # 24 and # 25 showed good continuity of results.

The results obtained from glass sample show the non-conductor properties very well as may be noted in Figure 26. The tabulated results of all tests performed on glass are recorded in Table 4. Since there are many different compositions of glass, direct comparison of results is rather difficult. Eckert[3] gives a value of $\epsilon_N = 0.94$ for glass at a temperature of 194°F and a value of $\epsilon_H = 0.88$ for the same temperature. These values are approximately 0.05 lower than those obtained in the tests but this difference may result because of a different composition as well as other errors in true surface temperature measurement. The amount of transmittance of energy at the low temperatures is negligible.

Values of ϵ_H / ϵ_N are given in Table 5. These results compare favourably with those of Eckert[3] given as 0.93 to 0.95.

Painted Copper

Two tests were performed on the painted copper surface at the same temperature and produced very uniform results. Temperature and emissivity values are recorded in Table 5. The emissivity values for Tests # 26 and # 27 are quite within the range of values given in the literature. Some published values of ϵ_N for flat black lacquer are 0.96 to 0.98 for a temperature range of 100°F to 200°F.[3,4] Another value range of ϵ_N for oil paints (all colors) is 0.92 to 0.96 for a temperature range of 212°F.[4]

Umir carried out a similar test at a slightly lower temperature on a flame oxidized copper plate painted with one coat of flat black enamel paint and obtained an ϵ_N of 0.87 and an ϵ_H of 0.83. The discrepancy would appear to be in the fact that the paint used was different and also only one coat was used rather than three.

The means by which the surface temperature was measured will be discussed in the conclusions of this report. Small errors in temperature measurement are involved and values of emissivities bear this out as compared to published results. Values of ϵ_H / ϵ_N are given in Table 6 and are in the expected range of 0.95 to 0.98. A directional plot for Test # 26 is shown in Figure 27.

TOTAL DIRECTIONAL EMISSIVITY FIG 21

A – TYPICAL NON-CONDUCTOR DIRECTIONAL EMISSIVE PROPERTIES

B – TYPICAL CONDUCTOR DIRECTIONAL EMISSIVE PROPERTIES

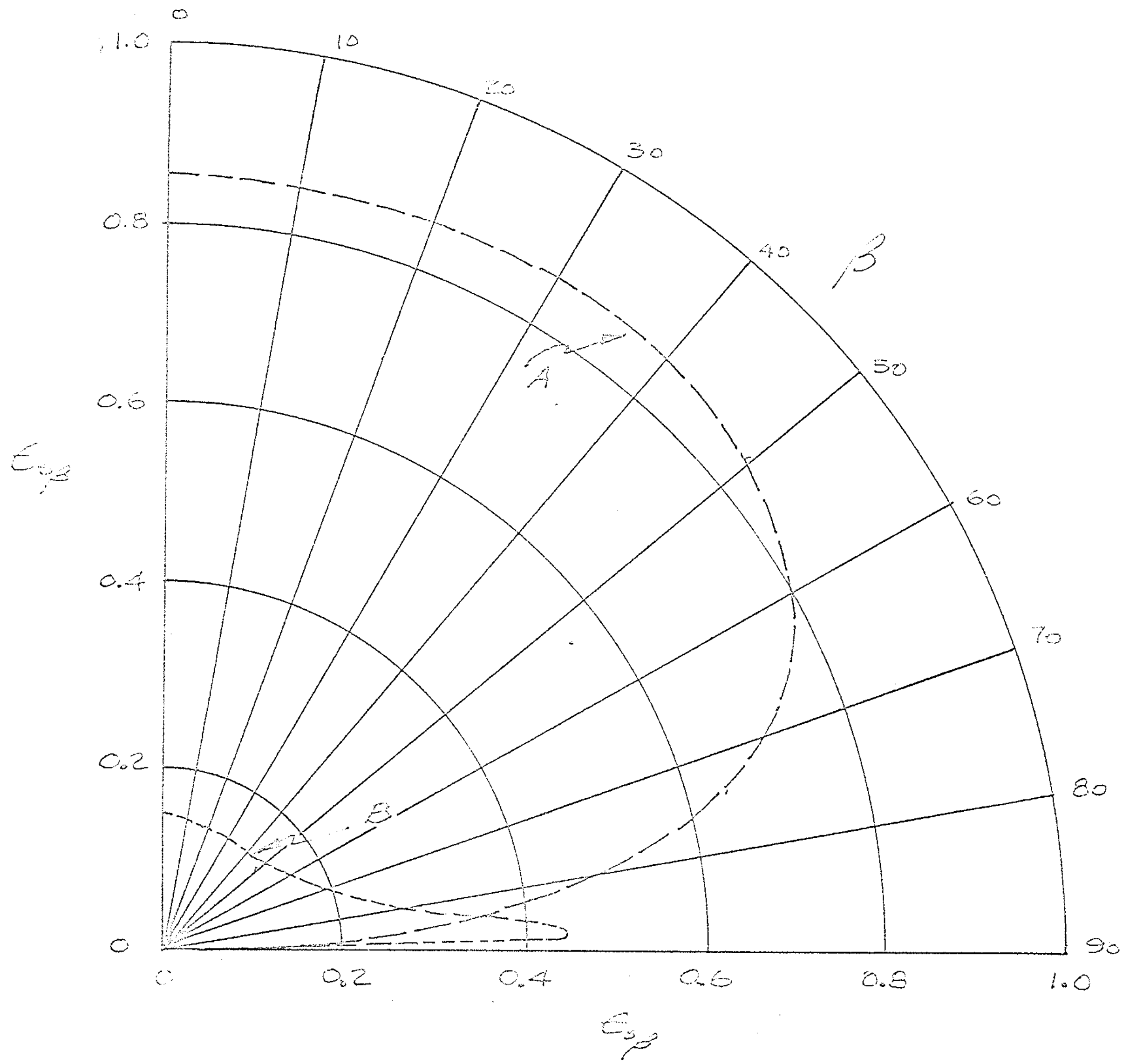

HAW/63

TABLE I

DIRECTIONAL EMISSIVITY

Sample - Copper

	Test Numbers			
Angle (°)	#1	#5	#6	#7
0	0.061	0.449	0.443	0.436
10	0.055	0.443	0.423	0.430
20	0.058	0.448	0.423	0.431
30	0.058	0.454	0.445	0.442
40	0.061	0.459	0.458	0.441
50	0.058	0.464	0.443	0.445
60	0.058	0.439	0.449	0.447
65	0.064	0.482	0.445	0.439
70	0.070	0.468	0.443	0.427
75	0.079	0.437	0.421	0.421
80	0.102	0.379	0.393	0.379
82	0.122	0.344	0.367	0.351
0	0.070	0.485	0.425	0.433
Temp (°F)	202	735	199	391

TOTAL DIRECTIONAL EMISSIVITY . FIG 22.

TEST #1

SAMPLE - COPPER

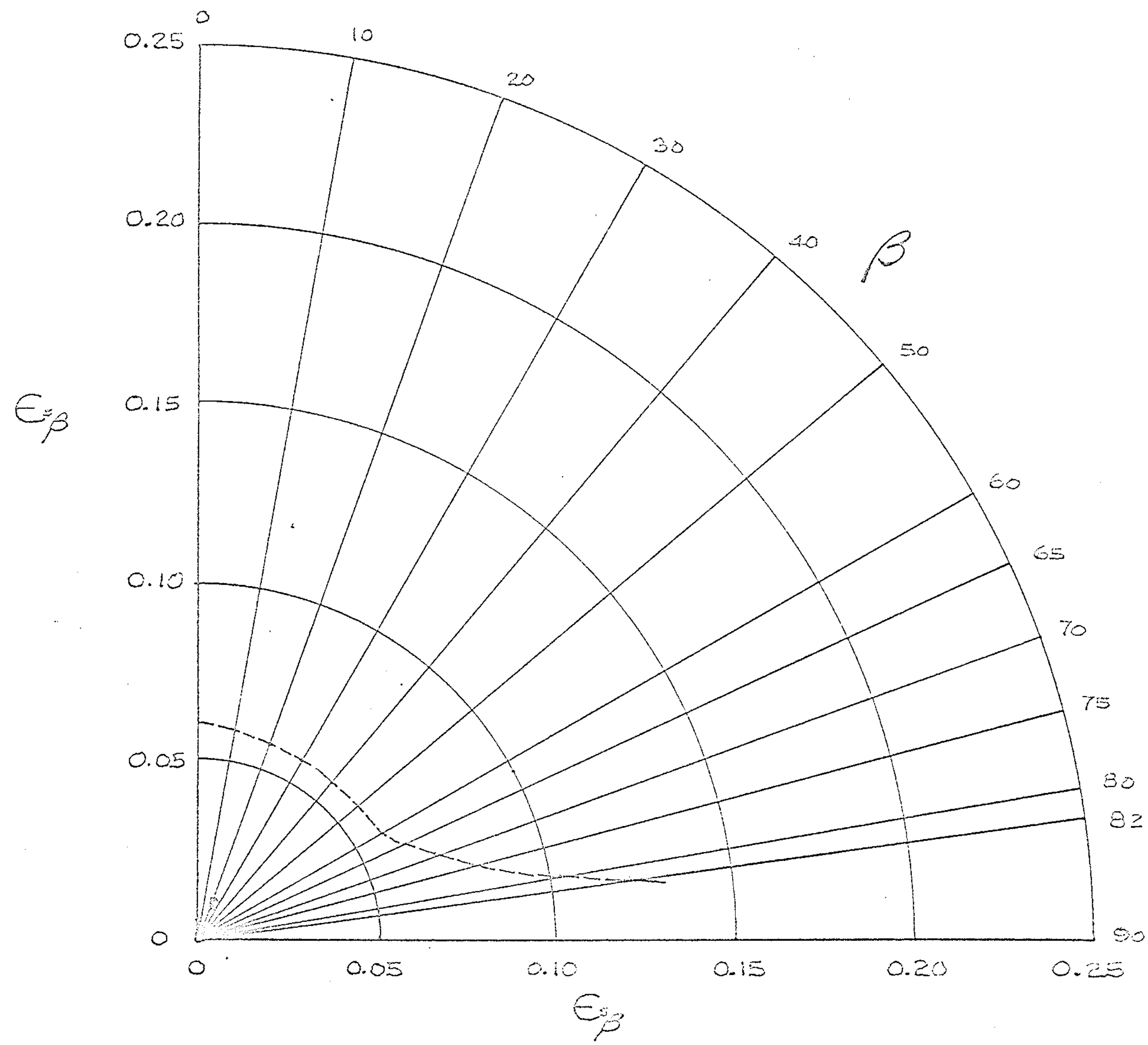

KAH./63

TOTAL DIRECTIONAL EMISSIVITY FIG 23

TEST # 5
SAMPLE - COPPER

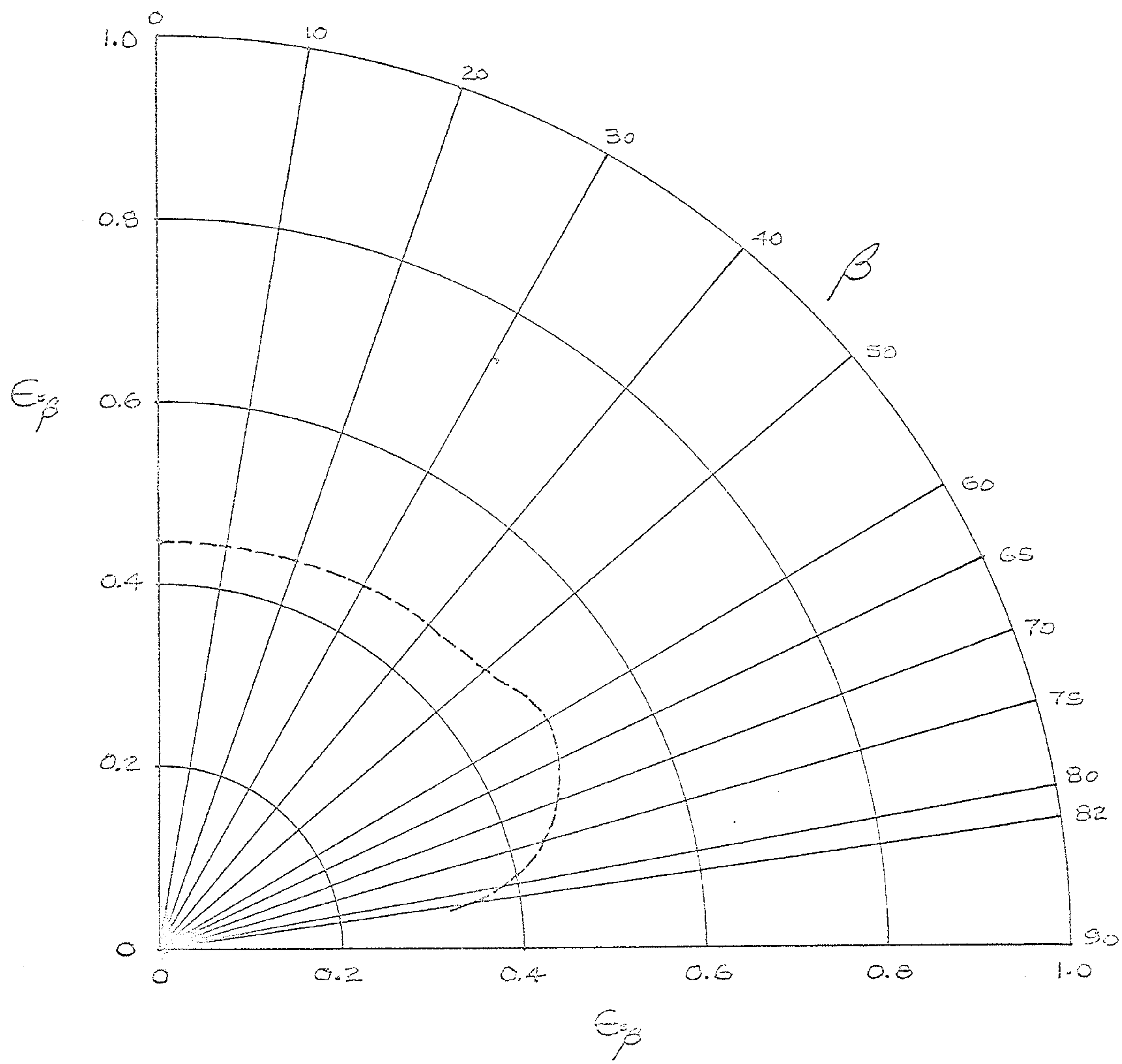

KAN/63

TABLE 2

DIRECTIONAL EMISSIVITY

Sample – Aluminum

	Test Numbers						
Angle (°)	#8	#9	#10	#11	#12	#13	#14
0	0.141	0.129	0.135	0.146	0.156	0.119	0.106
10	0.127	0.111	0.128	0.140	0.150	0.113	0.104
20	0.125	0.107	0.127	0.140	0.150	0.116	0.104
30	0.120	0.112	0.128	0.142	0.152	0.114	0.103
40	0.120	0.117	0.129	0.143	0.156	0.124	0.106
50	0.127	0.116	0.133	0.147	0.161	0.129	0.112
60	0.129	0.133	0.145	0.161	0.172	0.140	0.120
65	0.144	0.152	0.158	0.175	0.184	0.154	0.132
70	0.168	0.155	0.175	0.193	0.202	0.169	0.142
75	0.196	0.187	0.202	0.222	0.227	0.193	0.158
80	0.226	0.223	0.236	0.256	0.253	0.220	0.189
82	0.234	0.245	0.255	0.270	0.265	0.236	0.217
0	0.129	0.138	0.137	0.145	0.149	0.123	0.104
Temp (°F)	210	205	432	614	836	415	209

TOTAL DIRECTIONAL EMISSIVITY FIG 24

TEST #10

SAMPLE - ALUMINUM

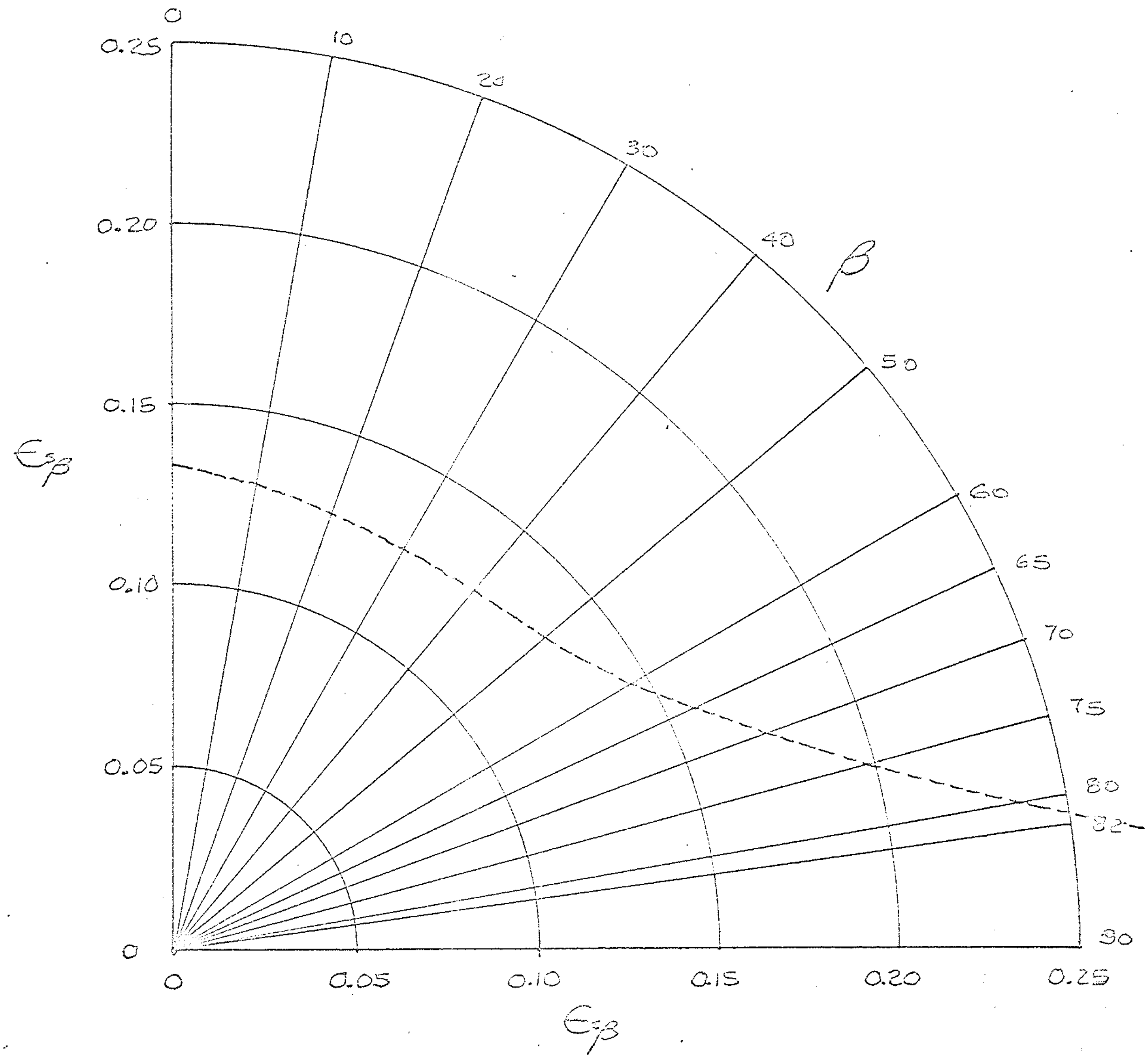

HAH/63

TABLE 3

DIRECTIONAL EMISSIVITY

Sample - Aluminum Foil

	Test Numbers				From Eckert
Angle (°)	#15	#16	#17	#18	and Drake (3)
0	0.051	0.030	0.033	0.039	0.039
10	0.041	0.026	0.028	0.033	0.039
20	0.038	0.025	0.029	0.033	0.038
30	0.036	0.025	0.030	0.032	0.038
40	0.034	0.027	0.031	0.032	0.040
50	0.044	0.028	0.033	0.035	0.043
60	0.051	0.032	0.036	0.039	0.050
65	0.052	0.035	0.040	0.042	- -
70	0.051	0.039	0.046	0.051	0.064
75	0.067	0.048	0.057	0.060	- -
80	0.085	0.067	0.077	0.077	0.100
82	0.105	0.078	0.091	0.086	- -
0	0.043	0.030	0.034	0.039	- -
Temp (°F)	206	398	628	200	Around 300°F

TOTAL DIRECTIONAL EMISSIVITY FIG 25

TEST # 15

SAMPLE - ALUMINUM FOIL

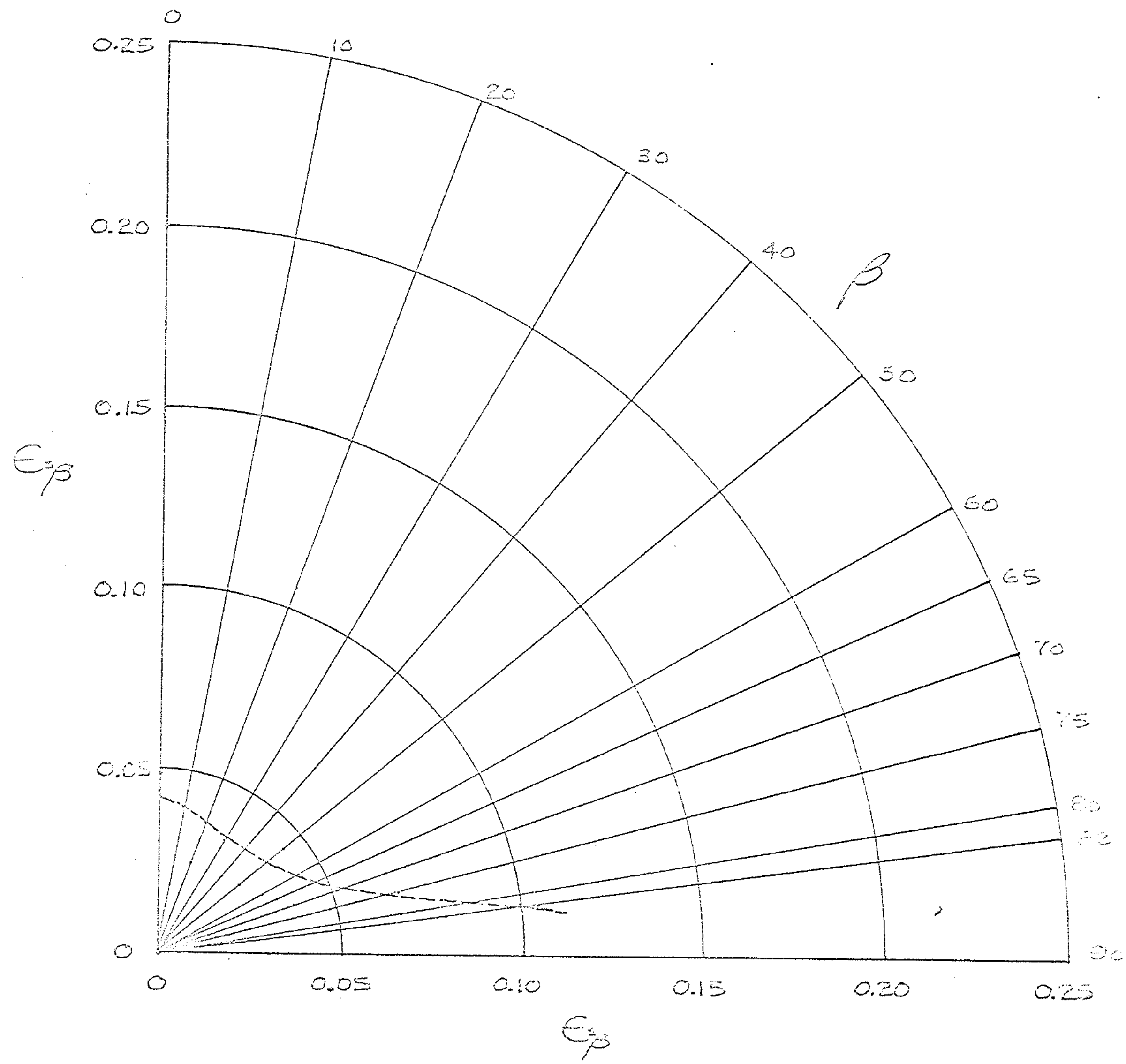

HAH./63

TABLE 4

DIRECTIONAL EMISSIVITY

Sample - Glass

Angle (°)	Test Numbers #19	#23	#24	#25
0	1.004	0.974	0.991	1.001
10	0.986	0.955	0.982	0.987
20	0.983	0.956	0.978	0.979
30	0.983	0.958	0.960	0.977
40	0.972	0.951	0.956	0.993
50	0.951	0.941	0.930	0.974
60	0.905	0.906	0.882	0.928
65	0.872	0.885	0.839	0.890
70	0.830	0.822	0.791	0.835
75	0.737	0.731	0.723	0.746
80	0.605	0.610	0.604	0.606
82	0.538	0.546	0.530	0.529
0	0.990	0.995	0.978	0.976
Temp (°F)	186	193	136	244

TOTAL DIRECTIONAL EMISSIVITY FIG 26

TEST # 24

SAMPLE – GLASS

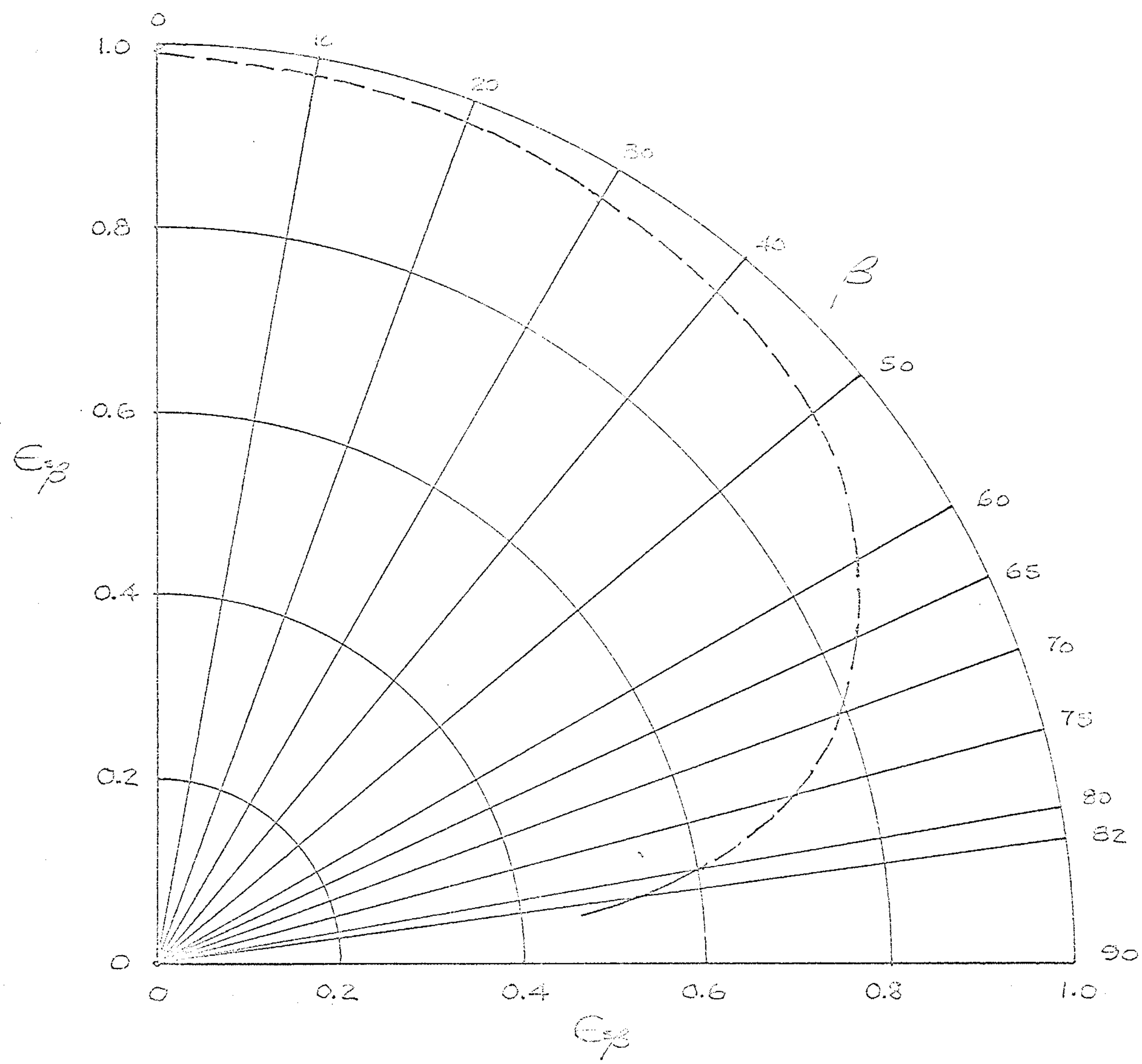

KAH./63

TABLE 5

DIRECTIONAL EMISSIVITY

SAMPLE-PAINTED COPPER

Angle (°)	Test Numbers # 26	# 27
0	0.950	0.957
10	0.948	
20	0.968	0.960
30	0.908	
40		0.987
50	0.950	
60	0.946	0.948
70	0.895	0.878
80	0.732	0.707
80	0.700	
0	0.974	0.985
Temp(°F)	178	178

TOTAL DIRECTIONAL EMISSIVITY FIG 27

TEST NO 26

SAMPLE - PAINTED COPPER

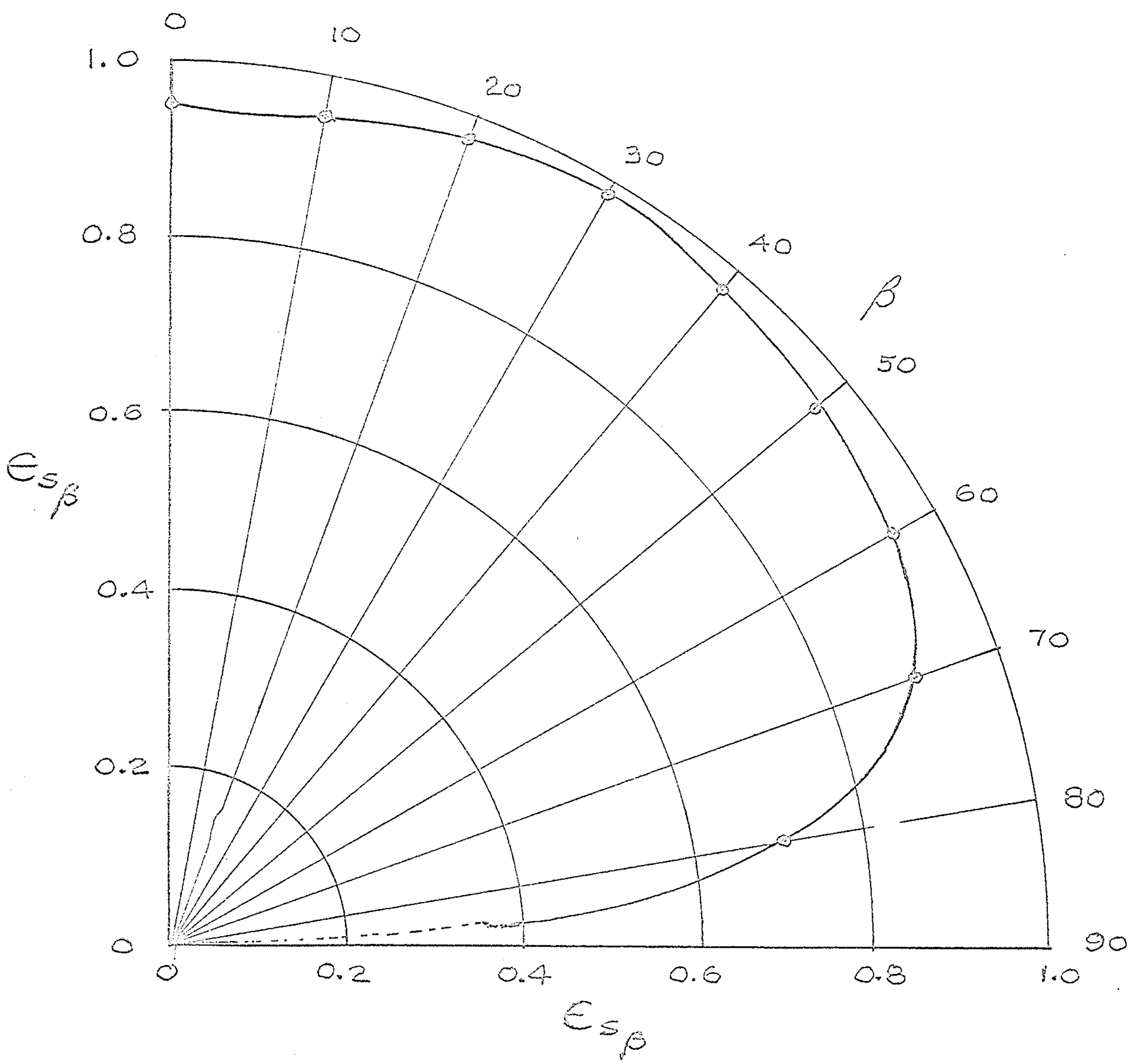

TABLE 6

HEMISPHERICAL AND NORMAL EMISSIVITIES

Test No.	Area in^2	K	$\epsilon_H = 2 \times Area \times K$	ϵ_N	ϵ_H / ϵ_N
1	9.03	0.00349	0.063	0.060	1.050
5	6.57	0.0349	0.459	0.450	1.020
6	6.32	0.0349	0.441	0.426	1.035
7	6.20	0.0349	0.433	0.435	0.995
8	9.71	0.00698	0.136	0.133	1.023
9	9.17	0.00698	0.128	0.128	1.000
10	10.43	0.00698	0.146	0.137	1.066
11	11.27	0.00698	0.157	0.144	1.090
12	12.25	0.00698	0.171	0.156	1.096
13	9.62	0.00698	0.134	0.122	1.098
14	8.56	0.00698	0.119	0.112	1.063
15	6.37	0.00349	0.044	0.040	1.100
16	4.55	0.00349	0.032	0.028	1.143
17	5.30	0.00349	0.037	0.032	1.156
18	5.78	0.00349	0.040	0.035	1.143
19	6.61	0.0698	0.923	0.990	0.932
23	6.66	0.0698	0.930	0.970	0.959
24	6.50	0.0698	0.907	0.986	0.920
25	6.64	0.0698	0.927	0.990	0.936
26	26.45	0.01732	0.921	0.950	0.968
27	26.53	0.01732	0.925	0.958	0.965

IX CONCLUSIONS

Results

The results of the tests clearly show that the emissivity is dependent on the angle of emittance and the type of material being considered. Conductors and non-conductors show definite directional characteristics by which they may be easily indentified. The tests demonstrated that, depending on the surface conditions, a material may yield results which may be associated with either or both types of material.

General trends in the emissivity with respect to its temperature dependency have not been well established because of the number of tests run and the type of material used. In one series of tests, the aluminum showed definite increase in directional emissivity values with an increase in temperature. The fact that there was some increase is characteristic of metallic surfaces and is exemplified by Equation (10) which was proposed by Schmidt and Eckert.[3] Only two specific results were calculated for copper and aluminum using Equation (10) and both values were lower than test or published results. Results obtained from Equation (10) would compare more favourably with emissivity values for completely unoxidized surfaces.[10] No such condition existed during the test procedure. Comparing individual results, the values for aluminum and aluminum foil show the best agreement with published results. Values obtained for copper are difficult to check because of the extreme dependency of emittance on the copper oxide formation on the surface.

The emissivity values for glass at low temperatures differ by about 0.05 from the published results. As explained previously it was believed that these results were as reliable as those for the other specimens. The differences may be due to a difference in composition between the glass tested and that for which comparative results were obtained. Secondly, of course, there is some experimental error. Here again, this error is believed to be of no greater significance than it is for the other results cited, the only possible differences occurring in surface temperature measurement. Stringent restrictions must be placed on these results as only applying to the temperature range mentioned.

The results for the painted copper surface agree closely with published results. The fact that the radiating surface is a non-conducting material is exemplified by its typical directional emissivity characteristics.

At this point some discussion on surface temperature measurement would seem apt. The boundary whose temperature was to be measured was an isothermal surface or considered so for most practical purposes. Placing thermocouples so as to measure the true surface temperature proved to be the most difficult task. Care was taken in each case to interfere as little as possible with any of the forms of heat transfer which took place. With the exception of the glass sample, all thermocouples were placed behind the surface whose emissivity was being measured. In the case of the glass sample, thermocouples were placed on the exposed surface and held in place by thermon which has a thermal conductivity much higher than glass but approximately the same emissivity.

All forms of heat transfer were relatively undisturbed.

In placing each thermocouple, a short to medium length of lead was placed on the surface or beneath the surface and the junctions were held firmly in place by thermon. This method was chosen over other methods such as peening, soldering or welding the thermocouples directly to the material. The practice of peening has proven quite satisfactory in many cases.

All samples tested, except glass, had a medium to high thermal conductivity. This tends to elliminate any thermal gradients which may exist on the sample surface and also produces small temperature gradients through the sample in the direction of the heat flow. In the case of the glass sample, the test results considered were only for low temperature runs where the above conditions are kept to a minimum. This also applies to the painted copper surface. Considering the thermal resistance of the paint as in Appendix C and the power setting as recorded on the data sheet, if fifty per cent of the heat passed directly through the painted surface, the temperature drop across the paint film would be approximately 2.3°F. The effect of this error is shown in the error analysis.

The effects of radiation absorption caused by water vapour in the air was considered negligible. The main reason for this assumption is the fact that relative measurements were considered rather than absolute values. The absorptivity of the water vapour depends on, the temperature of the water vapour, the product of the partial pressure of the water vapour and the depth of the layer, the partial pressure and total pressure prevailing. Gases and vapours need great thickness in order to absorb any major part of the incident radiation. Because of the design of the apparatus, the distances between radiating surfaces and the receiver were kept to a minimum and remained the same throughout all the tests. Variations in the pressures mentioned previously were small. It is also known that absorption occurs in only certain regions of the infrared spectrum. Taking into consideration all these factors, it is assumed that the error introduced by any vapour absorption would be negligible in comparison to other errors inherent in the results. One reference(2) quotes the fact that the water absorption added less than ± 0.5% error to his results.

Total hemispherical emissivities and ratios of ϵ_H to ϵ_N fall within the range of published data. To obtain a true value of the total hemispherical emissivity one should perform tests throughout a 360° rotation of the sample with respect to the vertical plane of sample rotation. It is possible that the emissivity could change as the direction of surface finish or structure is changed with respect to the viewing position.(1)

In Appendix D it is shown that the theoretical absolute error was ± 7.1%. The two greatest components of this error are caused by the sample temperature and the black body temperature. The actual guard temperature could be determined. This would involve certain difficulties which were previously encountered in surface temperature measurements. At higher temperatures the effect of the guard temperature is reduced because of the fourth power relationship. Since the error caused by the guard temperature is always in the same direction, its effect on the results is not as notable because it appears in both the top and bottom terms of the emissivity expression. This is particularly true when the sample temperature and the black body temperature are of similar magnitude or both high compared to the guard temperature. The error in the black body temperature which generally varies by about 6°F from front to back of the black body for an average temperature of 270°F must be tolerated. The variation in this temperature could be reduced by certain means as mentioned under apparatus performance.

Some zero drift of the thermopile readings occurred while water temperature fluctuations caused prolonged test time. Under all the foregoing adverse conditions it is conceded that the error could reach the 10 to 12% mark. Every effort was made to eliminate this possibility. The tests were manipulated as carefully as possible in order to keep experimental error to a minimum. Other similar projects have quoted theoretical errors in the order of 4% to 10% for their results and have excellent reproducibility.

The reproducibility of the results was very satisfactory. The average reproducibility for copper, painted copper and glass samples is 0.02 and for the aluminum 0.015. Except for two values at high angles, the aluminum foil results reproduce to within 0.01. It is concluded that the apparatus and test results have proven to be a success and the apparatus will prove to be of utmost benefit in further investigations.

Apparatus Performance

In general the apparatus performed satisfactorily with very few major obstacles being encountered. In order to improve the operation of the set-up, one of the first considerations should be given to obtaining a constant temperature bath, especially for use in conjunction with the radiometer. Any temperature variations over $\pm \frac{1}{2}^{\circ}F$ cannot be tolerated in the water temperature if it is used as a cooling medium for the radiometer. If this constant temperature bath were available, it would only be necessary to construct a water jacket which fit snug around the outside of the thermopile case. The present back of the thermopile case could be removed and the new water jacket would form the back. The prime consideration in this type of construction is to eliminate any air pockets between the thermopile case, and the jacket. This was one of the drawbacks of the first water jacket that was made. With a constant temperature bath, a thermopile water jacket and adequate shielding, the reliability and reproducibility of the radiometer could be greatly improved.

Some experimental error is involved in the temperature gradient which exists in the main black body. This error would increase at higher temperatures. To eliminate this problem it would be necessary to remove the end heater from its present position and reposition it on the open end of the black body. By having the two heaters controlled as they are at present, by variacs, it would only be a matter of adjusting the end heater to compensate for the temperature gradient towards the front of the black body. More insulation may also be added. It should not be difficult to reduce any difference to a maximum of 1 or $2^{\circ}F$. In order to verify any discrepancy in the guard temperature, several thermocouples would have to be carefully placed to read the surface temperature of the paint film without recording error due to radiation received from the sample or sample holder which is usually at a high temperature.

Generally, small error is involved in surface temperature measurements particularly at low temperatures and low heat fluxes. Assumptions made in the radiometer energy analysis were assumed to be valid and introduced negligible error. The main black body emissivity is believed to be equal to 0.98 or greater. The auxilliary black body is believed to be near perfect. The inside of the guard container is assumed to approach an isothermal enclosure with an emissivity of 0.92. It must be noted that copper was used instead of brass when testing the emissivity of the paint. This is believed to have no bearing on the results and using copper helped to reduce any temperature gradients in the backing plate next to the paint. Other indeterminate errors that have not been mentioned are considered negligible in comparison to those accounted for.

The remainder of the equipment performed satisfactorily. The guard sample holder and heater worked well. The angle measuring device was accurate and easy to manipulate. The fact that few and reliable instruments were utilized, tended to simplify the testing procedure. It must be kept in mind that each sample should be prepared carefully and a sufficient number of thermocouples positioned to give a good and accurate value of the surface temperature. Particular care must be taken when endeavouring to measure temperatures of materials which have very low thermal conductivity. It is thus surmised that with the foregoing improvements implemented and sufficient care taken, the apparatus would yield minimum error results with the maximum simplicity in procedure and operation.

BIBLIOGRAPHY

1. Talbert, S.G., "An Experimental Investigation of the Directional Emissivity Characteristics of Porous Metals," M.Sc. Thesis, University of Minnesota, December, 1959.

2. Umur, Aydin, "Measurement of Angular Emissivity," M.Sc. Thesis, Case Institute of Technology, May, 1953.

3. Eckert, E.R. G., Drake, Robert M., Heat and Mass Transfer, 2nd Edition, McGraw-Hill Book Co., New York, 1959.

4. McAdams, William H., Heat Transmission, 3rd Edition, McGraw-Hill Book Co., New York, 1954.

5. Giedt, Warren H., Principles of Engineering Heat Transfer, D. Van Nostrand Co., Princeton, N.J., June, 1958.

6. Schenck, Hilbert, Heat Transfer Engineering, Prentice-Hall Inc., Englewood Cliffs, N.J., 1959.

7. Buckley, H., "On Radiation from the Inside of a Circular Cylinder." Philosophical Magazine, 4, pp.753-762, 1927 ; 6, pp. 447 - 457, 1928 ; 17, pp. 576 - 581, 1934.

8. Barnes, B.T., Forsythe, W.E., Adams, E.Q., "The Total Emissivity of Various Materials at 100° - 500°C," Journal of the Optical Society of America, Vol. 37, # 10, October 1947.

9. Bedford, R.E., "A Low Temperature Standard of Radiation," Canadian Journal of Physics, Vol. 38, # 10, pp. 1256 - 1278, October,1960.

10. American Institute of Physics, Temperature, It's Measurement and Control in Science and Industry, National Bureau of Standards and National Research Council, Symposium, New York, November,1939.

11. Plank, Max., The Theory of Heat Radiation, Dover Publications, Inc., New York, 1959.

12. Kreith, Frank, Principles of Heat Transfer, International Textbook Co., Scanton, Pa., 19

13. Zimmerman, F.J., "Total Emissivities and Absorptivities of Some Commercial Surfaces at Room and Liquid Nitrogen Temperatures", Journal of Applied Physics, Vol. 26, # 12, pp. 1483-1488, December 1955.

14. Wood, W.D., Deem, H.W., Lucks, C.F., "Emissivity and Emittance," Batelle Memorial Inst. - DMIC Memorandum 72, 17, p. November 10, 1960.

15. Houghton, J.T., Brewer, A.W., "New Radiometer," Journal of Scientific Instruments, Vol. 31, # 5, pp. 184 - 187, May 1954.

16. Gordon, R., "Instruments for Direct Measurement of Intense Thermal Radiation," Review of Scientific Instruments, Vol. 24, # 5, pp. 366-370, May 1953.

17. Houghton, F.C., Olson, Harold T., "Measurement of Surface Temperature," Temperature Its Measurement and Control in Science and Industry (Vol. 1), Phienhold Publishing Co., (1941).

APPENDIX A

APPENDIX A

THERMOCOUPLE LOCATIONS

No.	Location
1	Thermocouple positions 1 - 5 shown in Figure 11.
2	
3	
4	
5	
6	Front of black body (inside).
7	Front of black body (inside).
8	Thermocouples 8 - 11 placed evenly between front and back of black body (inside).
9	
10	
11	
12	Back of black body (inside).
13	Back of black body (inside).
14	Inlet water temperature to guard top.
15	Outlet water temperature from guard top.
16	Inlet water temperature to guard base.
17	Outlet water temperature from guard base.
18	Inlet water temperature to auxilliary black body.
19	Outlet water temperature from auxilliary black body.
20	Inlet water temperature to radiometer housing.
21	Outlet water temperature to thermopile housing.

22 Inlet water temperature to thermopile housing.

23 Outlet water temperature from thermopile housing.

Note: Thermocouple 8 gave an incorrect reading and 22 and 23 were not used because this particular water jacket was not utilized.

THERMOCOUPLE ARRANGEMENT FIG 28

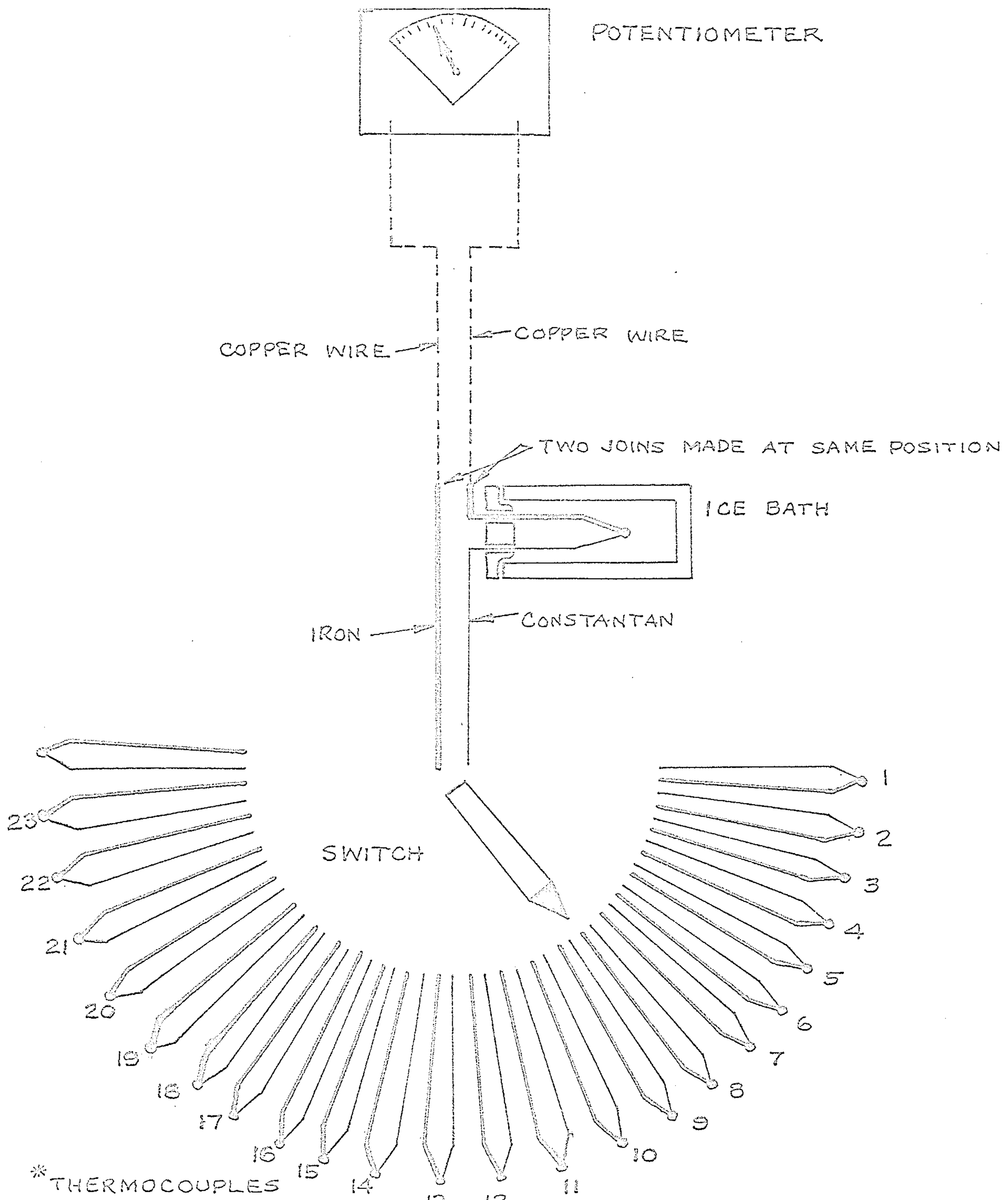

*THERMOCOUPLES
1-5 SAMPLE
6-13 BLACK BODY
14-23 WATER TEMPERATURES

* SEE ALSO APPENDIX A

UNIVERSITY OF MANITOBA
DEPT OF MECH. ENGINEERING
SCALE — NONE DATE JAN /64
DRWN HAH

APPENDIX B

APPENDIX B

SAMPLE CALCULATION

A sample calculation of Test # 18 is given to show the procedure in calculating the results for one directional emissivity test. The procedure is outlined as follows:

(1) All thermocouple emf's were averaged at each point. Temperatures were recorded to the nearest degree.

(2) The average temperatures were found for the sample, black body and guard. The guard temperature was taken as the average temperature between # 16 and # 17 thermocouples.

(3) Referring to data sheet # 1, the respective deflections, Δ, were taken directly as the readings given by the potentiometer. To compare the readings, they all had to be based on the same magnification factor.

To obtain the total hemispherical emissivity, values of $\epsilon_{S\beta}$ were first plotted on co-ordinate graph paper as shown in Graph # 1. A mean line was drawn through the points and the new values of $\epsilon_{S\beta}$ were read off the graph as listed below.

Referring to Equation (8) it should be noted that $\epsilon_{S\beta}$ may vary around the hemisphere. Since the sample was only tested at one value of θ, it must be assumed that $\epsilon_{S\beta}$ is constant around the hemisphere in order that a calculation may be performed. Thus Equation (8) breaks down as follows:

$$\epsilon_H = \frac{1}{\pi}\int_0^{\frac{\pi}{2}}\int_0^{2\pi} \epsilon_{\beta,\theta} \sin\beta \cos\beta \, d\beta \, d\theta \quad . \quad . \quad (8)$$

If ϵ_β constant with θ then:

$$\epsilon_H = 2\int_0^{\frac{\pi}{2}} \epsilon_\beta \sin\beta \cos\beta \, d\beta$$

$= 2$(Area under curve) Graph # 2.

The complete calculation is tabulated below:

β	$\epsilon_{S\beta}$	$\sin\beta \cos\beta$	$\epsilon_{S\beta} \sin\beta \cos\beta$
0	0.035	0	0
10	0.034	0.171	0.0058
20	0.033	0.321	0.0106
30	0.032	0.433	0.139
40	0.033	0.493	0.0163
50	0.036	0.493	0.0177
60	0.039	0.433	0.0169
70	0.050	0.321	0.0161
80	0.070	0.171	0.0132
90	0.000	0	0

A plot of $\epsilon_{S\beta} \sin\beta \cos\beta$ appears in Graph # 2. The area under the graph is 5.78 in^2. A constant must also be included to compensate for the scales used in plotting. One inch of the abscissa represents $20 \times \frac{\pi}{180}$ radians. One inch of the ordinate represents 0.01.

$$K = 20 \times \frac{\pi}{180} \times 0.01 = 0.00349$$

$$\epsilon_H = 2 \times 5.78 \times 0.00349$$

$$= 0.040$$

ϵ_N = 0.035 as estimated from Graph # 1.

$$\frac{\epsilon_H}{\epsilon_N} = \frac{0.040}{0.035} = 1.143.$$

Equation (10) from Eckert and Schmidt(3)

$$\epsilon_N = 0.576\sqrt{\rho_e t} - 0.124\ \rho_e\ t$$

ρ_e = electrical resistivity - ohm-cm

t = degrees Kelvin.

For copper at 202°F.

$$\rho_e = 1.724 + 75\ (0.00393) = 2.019 \times 10^{-6} \text{ ohm-cm.}$$

$$t = 368^\circ K$$

$$\epsilon_N = 0.576\sqrt{\frac{2.019 \times 368}{10^6}} - 0.124 \times \frac{2.019}{10^6} \times 368$$

$$= 0.155.$$

DIRECTIONAL EMISSIVITY MEASUREMENT

DEPT OF MECH ENG — SHEET # 1

TEST NO 18 SAMPLE ALUMINUM FOIL DATE JUNE 14/63

TIME A.M.	ANGLE	POTENTIOMETER SHIELD	SAMPLE	BL. BODY	THERMO COUPLES	TIME A.M. 1:40	2:23	TEMP	NOTES
1:50	0	0.390	50 0.641	50 5.228 100	1	4.82	4.85	198	
		0.438	0.630		2	4.90	4.93	200	
1:53	10	0.436	0.622		3	4.91	4.94	201	
		0.435	0.622		4	4.91	4.94	201	
1:56	20	0.408	0.597		5	4.87	4.90	199	$t_s = 200°$
		0.410	0.598		6	6.65	6.66	258	
2:00	30	0.400	0.602	5.289	7	6.67	6.68	259	
		0.411	0.581		8	—	—		
2:05	40	0.404	0.579		9	6.72	6.74	260	
		0.362	0.550		10	6.80	6.81	263	
2:07	50	0.352	0.540		11	6.84	6.86	264	
		0.340	0.551		12	6.84	6.85	264	
2:09	60	0.338	0.558	5.262	13	6.84	6.85	264	$t_B = 262°$
		0.328	0.550		14	1.13	1.11	72	
2:11	65	0.304	0.561		15	1.14	1.12	72	
		0.318	0.546		16	1.14	1.12	72	
2:12	70	0.272	0.582		17	1.14	1.13	72	$t_G = 72°F$
		0.301	0.582		18	1.14	1.13	72	
2:14	75	0.265	0.627		19	1.14	1.12	72	
		0.284	0.623		20	1.14	1.12	72	
2:16	80	0.278	0.740		21	1.14	1.12	72	
		0.302	0.748		22	—	—		
2:18	82	0.284	0.801		23	—	—		
		0.268	0.790	5.242					
2:20	0	0.290	0.517						
		0.278	0.512						

POWER SETTINGS BL. BODY MAIN HEATER 45 volts

END HEATER 0 volts

SAMPLE HEATER 15 %

ROOM TEMPS DRY 73°F RH 47%

WET 60°F

COMMENTS Test Satisfactory

DIRECTIONAL EMISSIVITY MEASUREMENT

DEPT OF MECH ENG

SHEET #1

TEST No 18 SAMPLE ALUMINUM FOIL

ANGLE	T_6-°R	T_5-°R	T_8-°R	T_6^4	T_5^4	T_8^4	$T_8^4-T_6^4$	$T_5^4-T_6^4$	$\frac{T_8^4-T_6^4}{T_5^4-T_6^4}$	Δ_6	$\Delta_{5/3}$	Δ_8	$\Delta_{5/3}-\Delta_6$	$\Delta_8-\Delta_6$	$\frac{\Delta_{5/3}-\Delta_6}{\Delta_8-\Delta_6}$	ϵ_{θ}
0	532	660	722	801	1897	2717	1.916	1.096	1.750	0.414	0.635	10.510	0.221	10.096	0.022	0.039
10										0.435	0.622		0.187	10.075	0.019	0.033
20										0.409	0.597		0.188	10.101	0.019	0.033
30										0.405	0.591		0.186	10.105	0.018	0.032
40										0.383	0.564		0.181	10.127	0.018	0.032
50										0.346	0.545		0.199	10.164	0.020	0.035
60										0.333	0.554		0.221	10.177	0.022	0.039
65										0.311	0.553		0.242	10.199	0.024	0.042
70										0.286	0.582		0.296	10.224	0.029	0.051
75										0.274	0.625		0.351	10.236	0.034	0.060
80										0.290	0.744		0.454	10.220	0.044	0.077
82										0.276	0.795		0.459	10.234	0.045	0.086
0										0.284	0.514		0.230	10.226	0.022	0.039

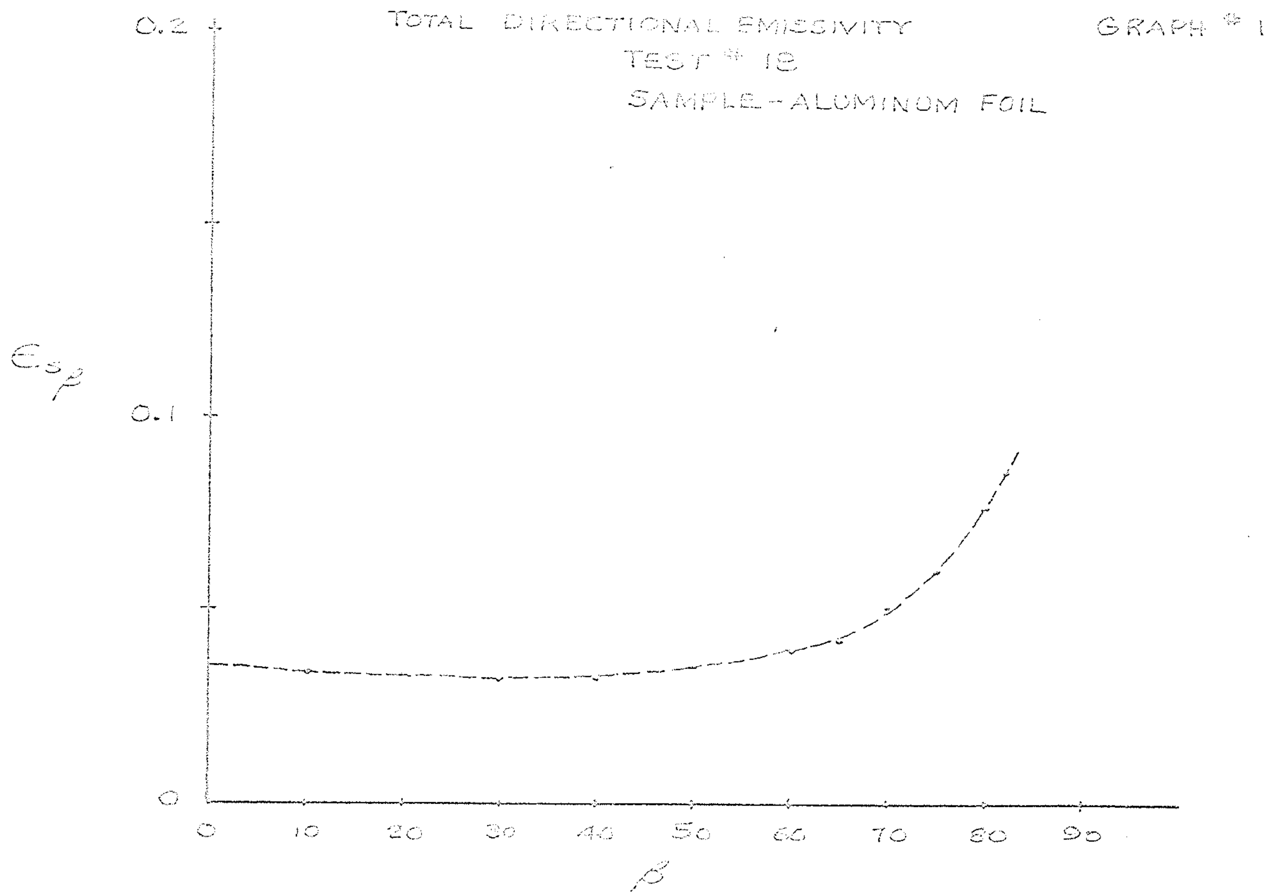
TOTAL DIRECTIONAL EMISSIVITY
GRAPH # 1
TEST # 18
SAMPLE - ALUMINUM FOIL
0.2
0.1
0
0
10
20
30
40
50
60
70
80
90
β

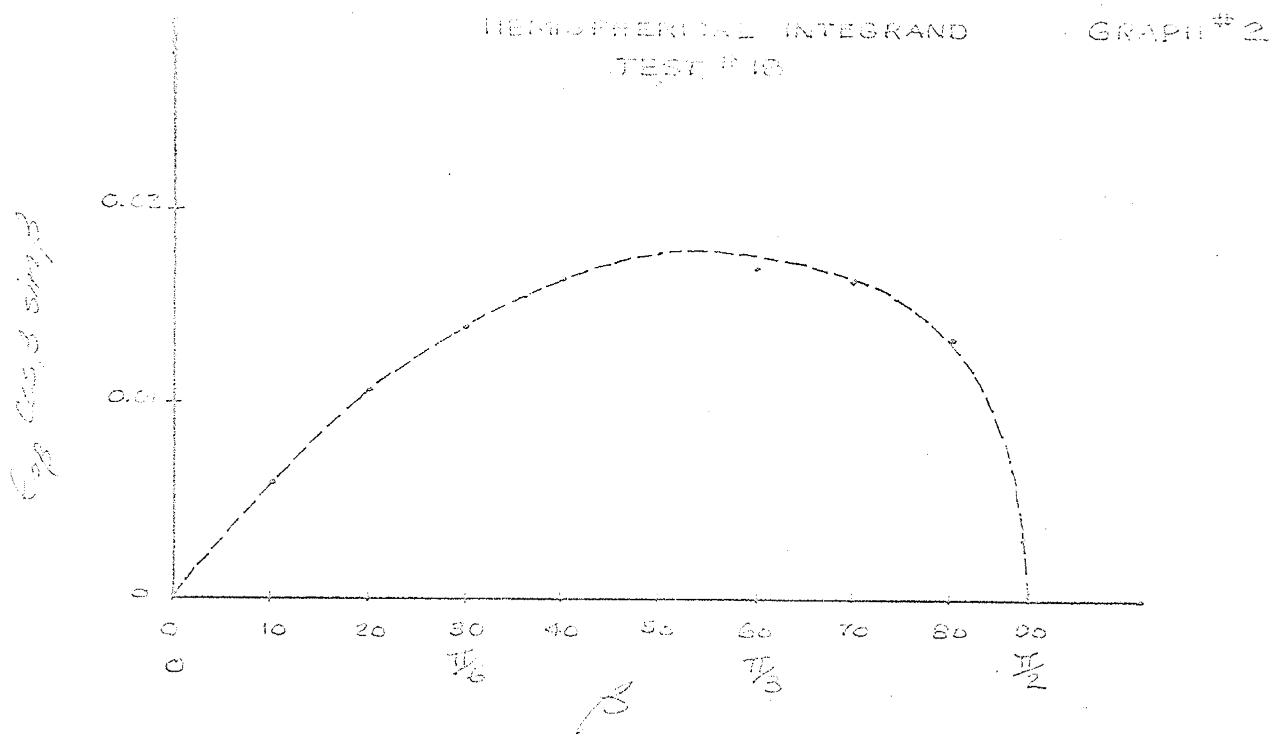
HEMISPHERICAL INTEGRAND
GRAPH # 2
TEST # 18
0.02
0.01
0
0
10
20
30
40
50
60
70
80
90
0
π/6
π/3
π/2
β

KAH/63

APPENDIX C

APPENDIX C

INSIDE GUARD CONDITIONS

In order to calculate the temperature distribution for the inside guard wall the convective coefficients for air side and water side must be known.

The inside air coefficient was estimated at 1 Btu/hr ft^2 ^oF.

From two equations from 'Eckert' the water side coefficient was calculated as 65 Btu/hr ft^2 ^oF.

$$k_1 (\text{brass}) = 60 \frac{\text{Btu}}{\text{hr-ft-}^oF}$$

$$k_2 (\text{paint}) = .58 \frac{\text{Btu}}{\text{hr-ft-}^oF}$$

This is the average of 3 values obtained from different references.

$$U = \frac{1}{\frac{1}{h_1} + \frac{x_1}{k_1} + \frac{x_2}{k_2} + \frac{1}{h_2}}$$

$$= \frac{1}{\frac{1}{65} + \frac{.0625}{60\text{x}12} + \frac{.020}{.58\text{x}12} + \frac{1}{1}}$$

$$= \frac{1}{.0154 + .0001 + .0029 + 1}$$

$$= \frac{1}{1.0184} = 0.982 \frac{\text{Btu}}{\text{hr-ft}^2\text{-}^oF}$$

Since the inside of the guard container has a hemispherical emissivity of 0.92 it is not unreasonable to assume that at least 80% of the heat exchange occurs by radiation

$$U \text{ for radiation} = \frac{1}{.0154 + .0001 + 0029}$$

$$= \frac{1}{.0184} = 54.5 \frac{\text{Btu}}{\text{hr-ft-}^oF}$$

Of all the tests run including those for the glass sample at the high temperatures the maximum setting of the sample heater was 45% or .45 x 2 kw which is 3070 Btu/hr.

To calculate temperature of paint surface Δt due to radiation

$$\Delta t_R = \frac{.80 \times 3070}{54.5 \times A}$$

$$A = \frac{2 \times \pi \times 7^2}{144} + \frac{\pi \times 14 \times 7}{144}$$

$$= 4.28 \text{ ft}^2$$

$$\Delta t_R = \frac{0.80 \times 3070}{54.5 \times 4.28} = 10.5^\circ F$$

$$\Delta t_C = \frac{0.0184}{1.0184} \times \frac{.20 \times 3070}{4.28 \times .982} = 2.7^\circ F$$

Therefore the inside guard temperature under these conditions is 13.7°F higher than the average water temperature passing through the guard.

This particular power setting was used on the glass sample at the high temperature test (over 800°F) of which the results were not taken. The next highest heat rate was for the copper sample at 735°F and a hemispherical emissivity of 0.46 which is about 45% of the heat given off as compared to glass. The temperature difference at this point would be approximately 6°F. The effect of any prevailing error of this nature is included in the error calculations Appendix D.

APPENDIX D

APPENDIX D

ERROR ANALYSIS

A theoretical error analysis is performed here for the conditions and results of test # 18. For this purpose each error is found by the procedure:

$$\text{Error} = \pm \left| \frac{\text{Avg. value} - \text{Extreme value}}{\text{Avg. Value}} \right|$$

The extreme value used is either the actual measured extreme or the possible calculated extreme whichever is greatest.

Repeating Equation (25)

$$\epsilon_{S\beta} = \frac{T_B^4 - T_G^4}{T_S^4 - T_G^4} \left[\frac{\Delta_S - \Delta_G}{\Delta_B - \Delta_G} \right]$$

(a) T_G error is compensating due to appearance in both denominator and numerator. Variation of T_G based on calculation of Appendix C (i.e. $\frac{15}{45} \times 13.7^\circ$)

$$\therefore \quad \text{error} = \pm \left| \frac{\dfrac{7.22^4 - 5.36^4}{6.60^4 - 5.32^4} - \dfrac{7.22^4 - 5.32^4}{6.60^4 - 5.32^4}}{\dfrac{7.22^4 - 5.32^4}{6.60^4 - 5.32^4}} \right|$$

$$= \pm \left| \frac{1.725 - 1.746}{1.746} \right|$$

$$= \pm \quad 1.2\%$$

(b) T_B error: in $T_B^4 - T_G^4$

$$= \pm \left| \frac{(7.22^4 - 5.32^4) - (7.18^4 - 5.32^4)}{(7.22^4 - 5.32^4)} \right|$$

$$= \pm \left| \frac{1916 - 1857}{1916} \right|$$

$$= \pm \left| \frac{59}{1916} \right|$$

$$= \pm \quad 3.1\%$$

(c) T_S error in $T_S^4 - T_G^4$

$$= \pm \left| \frac{(6.60^4 - 5.32^4) - (6.58^4 - 5.32^4)}{(6.60^4 - 5.32^4)} \right|$$

$$= \pm \left| \frac{1096 - 1075}{1096} \right|$$

$$= \pm \quad 1.9\%$$

(d) $\triangle_{S\beta} - \triangle_G$

$$\text{Error} = \pm \left| \frac{0.225 - 0.230}{0.225} \right|$$

$$= \pm \quad 2.2\%$$

(e) $\triangle_B - \triangle_G$

$$\text{Error} = \pm \left| \frac{10.168 - 10.075}{10.168} \right|$$

$$= \pm \quad 0.9\%$$

$$\text{Total theoretical error} = 1.2 + 3.1\% + 1.9 + 0.9$$
$$= \pm 7.1\%.$$

The theoretical error should indicate the maximum possible error in the determinations and the example chosen is representative of a worst condition.